N-(3-{4-[3-(trifluoromethyl)phenyl]piperazin-1-yl}propyl)-1*H*-indazole-3-carboxamide (D2AAK3) as a potential antipsychotic: *in vitro*, *in silico* and *in vivo* evaluation of a multi-target ligand

Agnieszka A. Kaczor[a,b*], Katarzyna M. Targowska-Duda[c], Piotr Stępnicki[a], Andrea G. Silva[d], Oliwia Koszła[a], Ewa Kędzierska[e], Angelika Grudzińska[a], Marta Kruk-Słomka[e], Grażyna Biała[e], Marián Castro[d]

[a] Department of Synthesis and Chemical Technology of Pharmaceutical Substances with Computer Modeling Laboratory, Faculty of Pharmacy, Medical University of Lublin, 4A Chodźki St., PL-20093 Lublin, Poland

[b] School of Pharmacy, University of Eastern Finland, P.O. Box 1627, FI-70211 Kuopio, Finland

[c] Department of Biopharmacy, Faculty of Pharmacy, Medical University of Lublin, 4A Chodźki St., PL-20093 Lublin, Poland

[d] Department of Pharmacology, Universidade de Santiago de Compostela, Center for Research in Molecular Medicine and Chronic Diseases (CIMUS), Avda de Barcelona, E-15782 Santiago de Compostela, Spain

[e] Department of Pharmacology and Pharmacodynamics, Faculty of Pharmacy, Medical University of Lublin, 4A Chodźki St., PL-20093 Lublin, Poland;

* Correspondence: agnieszka.kaczor@umlub.pl; Tel.: +48 81 448 7273

Abstract: Schizophrenia is a mental illness of not adequately understood causes that is not satisfactorily enough treated by current antipsychotics. In search for novel potential antipsychotics we performed structure-based virtual screening aimed to identify new dopamine D_2 receptor antagonists. We found compound D2AAK3 with affinity to dopamine D_2 receptor of 115 nM. D2AAK3 possesses additional nanomolar or low micromolar affinity to D_1, D_3, 5-HT_{1A}, 5-HT_{2A} and 5-HT_7 receptors, which makes it a good hit for further development as a multifunctional ligand. The compound has also some affinity to M_1 and H_1 receptors. We used homology modeling, molecular docking and molecular dynamics to study interactions of D2AAK3 with its molecular targets at the molecular level. In behavioral studies D2AAK3 decreases amphetamine-induced hyperactivity (when compared to the amphetamine-treated group) measured as spontaneous locomotor activity in mice. In addition, passive avoidance test demonstrated that D2AAK3 improves memory consolidation after acute treatment in mice. Elevated plus maze tests indicated that D2AAK3 induces anxiogenic activity 30 minutes after acute treatment, whereas this effect has no longer been observed 60 minutes after administration of the studied compound in mice.

Keywords: antipsychotics; central nervous system diseases; dopamine receptors; G protein coupled receptors; schizophrenia; serotonin receptors.

Abbreviations

5-CT, 5-carboxamidotryptamine; 5-HT, 5-hydroxytryptamine; 8-OH-DPAT, 8-hydroxy-2-(di-n-propylamino)tetralin; cAMP, Cyclic adenosine monophosphate; CHO-K1, Chinese hamster ovary K1; EPM, Elevated Plus Maze; Ecl1, Extracellular loop 1; Ecl2, Extracellular loop 2;

GPCRs, G protein-coupled receptors; HEK293, Human embryonic kidney 293; i.p., intraperitoneal; IL, Index of latency; IP, Inositol phosphate; MD, Molecular dynamics; NCI, Non-covalent interactions; ND, Not determined; PA, Passive avoidance; POPC, 1-palmitoyl-2-oleoyl-sn-glycero-3-phosphocholine; s.c., subcutaneous; SEM, Standard error of the mean; SP, Standard Precision

1. Introduction

Schizophrenia is a chronic and disabling mental disorder that affects how the person feels, thinks, and behaves. It is characterized by deficits in thought processes, perceptions, emotional responsiveness and likewise distortions in language, sense of self and behavior. It often includes psychotic experiences, such as hearing voices and delusions. Schizophrenia begins typically in late adolescence or early adulthood (first symptoms are usually observed between the ages of 16 and 30) and is estimated to affect about 1% of the population. Mental disorders are the largest contributors to disability in young adults worldwide and schizophrenia has remained the 15th leading cause of years lived with disability (YLDs) among the global population over the last three decades (GBD 2017 Disease and Injury Incidence and Prevalence Collaborators, 2018).

More than 50% of people with schizophrenia are not receiving appropriate care. 90% of people with untreated schizophrenia live in low- and middle-income countries. Lack of access to mental health services is an important issue. Furthermore, people with schizophrenia are less likely to seek care than the general population (O'Callaghan et al., 2010; Stępnicki et al., 2018). Untreated schizophrenia may lead to severe problems affecting various areas of life.

Complications caused or associated with schizophrenia include: suicide, thoughts of suicide and suicide attempts, anxiety disorders, depression, self-injury, abuse of other drugs or alcohol, inability to work, legal and financial problems, social isolation, homelessness, health problems, aggressive behavior, being victimized.

The causes of schizophrenia still remain unclear. They involve a combination of genetic and environmental factors – a person may be genetically predisposed to schizophrenia, but exposure to environmental factors, such as prenatal and perinatal stressors, childhood trauma, infectious agents, the urban environments, a lack of exposure to social interactions, socioeconomic status and life events, may be required to develop the disease. The main hypothesis to explain the pathomechanism of schizophrenia is based on the dopaminergic dysfunction. According to this hypothesis, changes in dopamine level in the mesolimbic pathway are associated with positive symptoms, whereas negative symptoms are related to changes in the mesocortical pathway. Other neurotransmitters considered to be involved in the pathogenesis of schizophrenia are glutamate and serotonin. Current treatment focuses on reducing symptoms of the disease. Antipsychotic drugs of the first generation act mainly as dopamine D_2 receptor antagonists. Second generation drugs are multi-target D_2 antagonists that possess additional and greater affinity for serotonin receptors, mainly 5-HT_{2A} receptor, while multifunctional antipsychotic drugs that show partial or biased agonism activity at D_2 receptors have been classified as third generation antipsychotics. Currently available antipsychotics have proven to be effective in reducing positive symptoms, such as hallucinations, delusions and thought disorders, but their effectiveness is lesser on negative symptoms such as social

withdrawal, apathy and motivation problems as well as on cognitive impairments (Barnes et al., 2020; Stępnicki et al., 2018).

The pathomechanism of complex diseases, such as schizophrenia, usually involves several different neurotransmitters and in such conditions selective drugs often turn out to be insufficiently effective. For a long time, the classical model of drug action where one medicine ("magic bullet") targets one receptor was pursued as it was considered to be better than the model of non-selective drugs. It was due to presumption that drugs affecting only one certain receptor cause fewer side effects than in case of targeting several different receptors. However, in some complex conditions magic bullets are ineffective and hence scientists now focus on searching for multi-target drugs ("shotguns"), which fit to a number of receptors involved in the pathomechanism of a disease. In schizophrenia, the affinity for different aminergic GPCRs of multi-target agents may contribute to clinical efficacy on the different symptoms domains of the illness and cause fewer side effects comparing to more selective, first generation, drugs. Therefore, a tailored multi-target profile is currently desired for future, better antipsychotics.

In order to identify novel ligands of dopamine D_2 receptor, structure-based virtual screening was performed (Kaczor et al., 2016c). As a result of these studies, among others, compound D2AAK3 (Fig. 1) was found as a dopamine D_2 receptor antagonist, with an affinity of 115 nM for this receptor. Moreover, the compound exhibits nanomolar or low micromolar affinity also for D_1, D_3, 5-HT_{1A}, 5-HT_{2A} and 5-HT_7 receptors, what fulfills the assumptions of multi-target paradigm in drug discovery and makes D2AAK3 a promising candidate for a further development as a novel antipsychotic. Thus, we took a closer look at the properties of

the found virtual hit. To assess interactions of the identified compound with its targets at the molecular level, different techniques of molecular modeling, such as homology modeling, molecular docking and molecular dynamics, were performed. *In vivo* studies were carried out in order to evaluate antipsychotic properties of D2AAK3 and its impact on memory consolidation and anxiety-like behavior in mice.

2. Material and Methods

2.1. *In vitro* studies

2.1.1. Receptor binding assays

Radioligand binding assays were performed on cell membrane preparations from cell lines stably expressing the human cloned receptors. Chinese hamster ovary K1 (CHO-K1) cell lines stably expressing human D_{2S}, 5-HT_{2A} or H_1 receptors and human embryonic kidney 293 (HEK293) cell lines stably expressing human 5-HT_{1A} or 5-HT_7 receptors were in-house available (Kaczor et al., 2016c; Varin et al., 2010), whereas CHO-K1 cell lines stably expressing human D_1 or D_3 receptors (Perkin Elmer, Waltham, MA, USA) and Chem-1 cell line stably expressing human M_1 receptor (Millipore) were commercially available. 0.7 nM [^{3}H]-SCH23390 (D_1), 0.2 nM [^{3}H]-Spiperone (D_2), 1 nM [^{3}H]-Spiperone (D_3), 2 nM [^{3}H]-8-OH-DPAT (5-HT_{1A}), 1 nM [^{3}H]-Ketanserine (5-HT_{2A}), 2 nM [^{3}H]-SB269970 (5-HT_7), 2 nM [^{3}H]-Pyrilamine (H_1) and 2 nM [^{3}H]-Pirenzepine (M_1) were employed as radioligands. Non-specific binding was assessed in the presence of 1 μM butaclamol (D_1), 10 μM sulpiride (D_2), 1 μM haloperidol (D_3), 10 μM serotonin (5-HT_{1A}), 1 μM metisergide (5-HT_{2A}), 25 μM clozapine (5-HT_7), 10 μM triprolidine (H_1) and 200 μM pirenzepine (M_1). Competition binding

curves of compound D2AAK3 at the different receptors were constructed using six or seven different concentrations of compound, starting at 0.1 nM or 1 nM till full displacement or 100 μM as maximal concentration were reached. Affinity (equilibrium dissociation constant (K_i) and pK_i (-logK_i) values) were calculated using Prism 6 software (GraphPad, San Diego, CA), by fitting the data from competition binding curves to a single binding site competition model using the equations logEC50 = log(10^logKi*(1+HotNM/HotKdNM)) and Y = Bottom + (Top - Bottom)/(1+10^(XLogEC50)), where Y is binding, HotNM is the concentration of radioligand in the assay, HotKdNM is the equilibrium dissociation constant (K_d) of the radioligand as determined in saturation binding experiments, and X is the logmolar concentration of unlabelled compound.

2.1.2. Functional assay at D_2 receptors

The efficacy of D2AAK3 as agonist or antagonist of D_2 receptors was evaluated in functional assays of cAMP signaling in the CHO-K1 cell line stably expressing the human D_{2S} receptor employed in radioligand binding assays, following a protocol already described (Kaczor et al., 2016c, 2016d). Compound was initially assessed at 10 μM concentration either as agonist or as antagonist of 10 μM dopamine response. 10 μM dopamine was used as reference agonist in these assays. The potency (K_B) of the compound as D_2 antagonist was determined by Schild analysis of the effect of three different concentrations (150 nM, 1 μM and 10 μM) of compound on the concentration-response curves of the agonist quinpirole (Kenakin, 2014).

2.1.3. Functional assay at 5-HT_{1A} receptors

The efficacy of D2AAK3 as agonist or antagonist of 5-HT_{1A} receptors was evaluated in functional assays of cAMP signaling in the HEK293 cell line stably expressing the human 5-HT_{1A} receptor employed in radioligand binding assays, following a protocol already described (Kaczor et al., 2016d). Compound was assessed in concentration (0.1 nM – 100 μM)-response curves either as agonist or as antagonist of 3 nM 5-carboxamidotryptamine (5-CT) response. 5-CT (1 pM – 10 μM) and methiothepin (0.1 nM – 10 μM) were used in these assays as reference agonist and antagonist, respectively.

2.1.4. Functional assay at 5-HT_{2A} receptors

The efficacy of D2AAK3 as agonist or antagonist of 5-HT_{2A} receptors was evaluated in functional assays of inositol phosphate (IP) production in the CHO-K1 cell line stably expressing the human 5-HT_{2A} receptor employed in radioligand binding assays, following a protocol already described (Kaczor et al., 2016d). Compound was assessed in concentration (0.1 nM – 100 μM)-response curves either as agonist or as antagonist of 1 μM serotonin (5-HT) response. 5-HT (0.1 nM – 100 μM) and risperidone (0.01 nM – 10 μM) were used in these assays as reference agonist and antagonist, respectively.

2.2. Molecular modeling

2.2.1 Receptor structures

To perform molecular docking the available X-ray structures of studied receptors were downloaded from PDBdb, and subsequently modified (if necessary) with Schrödinger software v. 2019-4. In particular, dopamine D_2 receptor in complex with the antagonist risperidone (PDB

ID: 6CM4 (Wang et al., 2018)), dopamine D_3 receptor in complex with the antagonist eticlopride (PDB ID: 3PBL (Chien et al., 2010)), as well as serotonin 5-HT_{2A} receptor in complex with the antagonist risperidone (PDB ID: 6A93 (Kimura et al., 2019)). In case of dopamine D_1 (Kaczor et al., 2016d) and serotonin 5-HT_7 receptor (Kaczor et al., 2020) the homology models were used as previously reported. Modeller v. 9.14 (Webb and Sali, 2016) was used to construct a homology model of serotonin 5-HT_{1A} receptor in an active conformation. In this regard, the cryo-EM structure of serotonin 5-HT_{1B} receptor, in complex with an agonist donitriptan (PDB ID: 6G79), was used as a template (García-Nafría et al., 2018). For sequence alignment (Edgar, 2004) the MUSCLE (Multiple Sequence Comparison by Log-Expectation) was used (the sequence identity was 51% and sequence similarity 68%). Modeller v. 9.14 generated a population of 100 models. Based on Discrete Optimized Protein Energy (DOPE) profiles obtained from Modeller v. 9.14 software the best model was selected. In addition, the biomolecules structures were preprocessed using the Protein Preparation Wizard of Maestro Release 2019.4 to optimize the hydrogen bonding network as well as to remove any possible artifacts.

2.2.2. Compound preparation

D2AAK3 was modeled using LigPrep module of Schrödinger software v. 2019-4 as described previously (Kaczor et al., 2016c, 2016d, 2016a, 2020; Kondej et al., 2018a, 2019). To determine the protonation state, Epik module of Schrödinger software v. 2019-4 was used.

2.2.3. Molecular docking

For molecular docking of D2AAK3 to the studied receptor models Standard Precision (SP) approach of Glide from Schrödinger v. 2019-4 was applied as described previously (Kaczor et al., 2016c, 2016d, 2016a, 2020; Kondej et al., 2018a, 2019). For each receptor 100 poses were generated. Then, the final poses were chosen based on Glide docking scores and visual inspection of the poses that propose the interaction between the protonatable nitrogen atom of the ligand and conserved Asp 3.32. Maestro v. 2019.4 and PyMol v. 2.0.4 software were used to analyze the molecular modeling results. Non-covalent interactions maps of ligand-receptor interactions were computed with NCIPlot v. 3.0 (Contreras-García et al., 2011) at the distance below 4 Å from the ligand and subsequently visualized with VMD v. 1.9.1 (Humphrey et al., 1996).

2.2.4. Molecular dynamics

The D2AAK3-receptor complexes were subjected to molecular dynamics with Desmond v. 3.0.3.1 (Bowers, 2006) as described previously (Kaczor et al., 2016d, 2016a, 2020). Briefly, the complexes were embedded in POPC (1-palmitoyl-2-oleoyl-sn-glycero-3-phosphocholine) membrane, hydrated and ions were added in order to neutralize protein charges (to concentration of 0.15 M NaCl). The complexes were minimized and subjected to MD. In particular, first in the NVT ensemble (1 ns) and then in NPT ensemble (20 ns) with the protein backbone restrictions in each case. The production runs (200 ns) were performed in NPT ensemble with no restrictions.

2.3. *In vivo* studies

2.3.1. Animals

The experiments were carried out on 2 month old, naïve Swiss male mice (Farm of Laboratory Animals, Warszawa, Poland), weighing 20–30 g. All experiments were carried out according to the National Institute of Health Guidelines for the Care and Use of Laboratory Animals and the European Community Council Directive for Care and Use of Laboratory Animals (2010/63/*EU*) and approved by local ethics committee (license 2/2015) as reported earlier (Kaczor et al., 2016d). Mice were maintained under standard laboratory conditions and were adapted to the laboratory conditions as described perviously (Kaczor et al., 2016d).

2.3.2. Drugs

D2AAK3 was purchased from Enamine (Z373926824), d-amphetamine sulphate and saline (0.9% NaCl) from Sigma-Aldrich (St. Louis, MO, USA). D-amphetamine was dissolved in saline, D2AAK3 and MK-801 (Tocris, USA) were suspended in 1% Tween 80 and subsequently diluted in saline (0.9%, vehicle). D-amphetamine was injected subcutaneously (s.c.) and D2AAK3 was administered intraperitoneally (i.p.). D2AAK3, d-amphetamine, MK-801 and vehicle were freshly prepared before each experiment. Control groups received injections (vehicle) at the same volume and by the same route of administration as previously reported (Kaczor et al., 2020).

2.3.3. Motor coordination evaluated by rotarod and chimney tests

Motor coordination has been evaluated using the rotarod test and the chimney test based on the same procedures as described previously (Kaczor et al., 2016d). Both tests were

performed 60 min after injection of D2AAK3 (100 mg/kg; i.p.) (n = 7-8) or vehicle (i.p.) (n = 7-8), using the same group of mice (i.e., after rotarod test each mouse was placed to the chimney test).

2.3.4. Spontaneous locomotor activity and amphetamine-induced hyperactivity

D2AAK3 effect on mouse spontaneous locomotor activity was evaluated using an animal activity meter Opto-Varimex-4 Auto-Track (Columbus Instruments, USA), measured in a sound-attenuated experimental room. The Auto-Track System senses motion with a grid of infrared photocells monitoring animal movements. In particular, the arithmetic average of distance (cm) traveled by a mouse (± SEM) measured for each group were analyzed. Each mouse was placed to each cage for 60 min immediately after D2AAK3 (100 mg/kg; i.p.), amphetamine (5 mg/kg; s.c.) or vehicle (as a control). To determine whether D2AAK3 influence on amphetamine-induced hyperactivity, each mouse received D2AAK3 (100 mg/kg; i.p.) or vehicle and 30 min later amphetamine (5 mg/kg; s.c.) or vehicle injection and then spontaneous locomotor activity was recorded for 30 min.

2.3.5. Elevated plus maze (EPM) procedure

D2AAK3 effect on anxiety-like behavior in mice was determined using the elevated plus maze (EPM). The experimental apparatus was shaped like a “plus” sign and consisted of a central platform, two open arms opposite to each other and two equal-sized enclosed arms opposite to each other. The maze, made of dark Plexiglas, was illuminated by dim light and elevated to a height of 50 cm above the floor. The EPM procedure was described in our previous work (Kaczor et al., 2016d). The percentage (%) of time spent in the open arms and % of open

arm entries were determined. In addition, the closed arm entries were recorded as the indicator of mouse motor activity. In order to evaluate the acute injection of D2AAK3 on anxiety-like behavior the studied compound (100 mg/kg; i.p.) (n = 8-10) or vehicle (i.p.) (n = 8-10) was administered 30 and 60 minutes before the EPM test.

2.3.6. Passive avoidance (PA) task

D2AAK3 effect on long-term memory was evaluated in mice using the PA task. The PA apparatus consisted of two-compartment acrylic box, one illuminated with fluorescent light (8 W) and another darkened connected by a guillotine door. Entrance of the animal to the darkened box was punished by an electric foot shock (0.2 mA for 2 s). The PA procedure were described previously (Kaczor et al., 2016d). The animals received D2AAK3 (100 mg/kg; i.p.) or vehicle (control group) immediately after the PA test (Day 1), and those rodents were retested on Day 2 (24 h later). In a separate experiment, we provoked the schizophrenia-like behaviors (i.e., cognitive impairment correlating with the cognitive symptoms of schizophrenia in humans) in mice by an acute administration of MK-801 (0.3 mg/kg) (Kruk-Slomka and Biala, 2016). The animals received D2AAK3 (50 mg/kg; i.p.) immediately after the pretest (Day 1), and 15 min later MK-801. On the Day 2, the mice were retested as previously described. The changes in PA performance were expressed as the difference between retention (Day 2) and training (on Day 1) latencies (Kaczor et al., 2016d) and were presented as a latency index (IL). More specifically, IL was calculated for each animal and reported as the ratio as reported previously (Kaczor et al., 2016d).

2.3.7. Statistical analysis

The statistical analyses were performed by two-way analysis of variance (ANOVA) followed by the Newman-Keuls's post hoc test and t-test to compare the differences between the studied drug and control group. Data were presented as mean ± SEM. The confidence limit of $p<0.05$ was considered statistically significant.

3. Results

3.1. *In vitro* studies

3.1.1. Affinity profile of D2AAK3 at receptors of the antipsychotic receptorome

We have previously reported the affinities of compound D2AAK3 at selected dopaminergic (D_2, D_1 and D_3) and serotonergic (5-HT_{1A} and 5-HT_{2A}) receptor subtypes targeted by current antipsychotic drugs (Kaczor et al., 2016c) (Table 1), which were in the medium nanomolar range at 5-HT_{1A}, D_2 and 5-HT_{2A} receptors. Here we have undertaken an extended pharmacological profiling of D2AAK3 at other receptors from the GPCR receptorome considered relevant for clinical efficacy and/or side effects of antipsychotics, that is serotonin 5-HT_7, histamine H_1 and muscarinic M_1 receptors. D2AAK3 displayed moderate affinity at H_1 receptors and low affinity at 5-HT_7 receptors, whereas it did not show affinity for muscarinic M_1 receptors. Affinity (p*K*i, *K*i) values are given in Table 1. Examples of competition radioligand binding curves of D2AAK3 at the different receptors can be found in Supplementary Information, Fig. S1.

3.1.2. D2AAK3 is a D_2/5-HT_{2A} antagonist with agonist efficacy at 5-HT_{1A} receptors

We have previously characterized D2AAK3 as a competitive antagonist of D_2 receptors in *in vitro* cAMP assays of D_2 function (inhibition of forskolin-stimulated cAMP, cyclic

adenosine monophosphate, production) based on the results from Schild analysis (Kaczor et al., 2016c). The antagonistic effect of three different concentrations of D2AAK3 on the concentration-response curves of the D_2-like receptor full agonist quinpirole resulted in Schild plots with slope close to unity (-1.248; 95% Confidence Intervals -1.577 to -0.9191) and retrieved an antagonist potency of K_B = 131 nM (Kaczor et al., 2016c) (Table 2).

D2AAK3 was further functionally evaluated as agonist or antagonist of 5-HT_{1A} and 5-HT_{2A} receptors. In *in vitro* cAMP assays of 5-HT_{1A} function (inhibition of forskolin-stimulated cAMP production) in HEK293 cells expressing the human cloned receptor, the compound elicited a full agonist response (maximal response at the highest concentration evaluated (100 μM) of 92.6%), whereas it showed low agonist potency (EC_{50} = 4246 nM) (Fig. 2A) (Table 2).

The efficacy of D2AAK3 at 5-HT_{2A} receptors was investigated in *in vitro* assays of inositol phosphate production in CHO-K1 cells expressing the human cloned receptor. The compound was unable to promote IP (inositol phosphate) production at the concentrations assayed (from 10^{-10} to 10^{-4} M), indicating lack of agonist efficacy, while the control agonist 5-HT efficiently promoted IP production in a concentration-dependent manner (data not shown). On the contrary, D2AAK3 (from 10^{-10} to 10^{-4} M) fully antagonized the 5-HT (1 μM)–mediated IP production in a concentration-dependent manner, with an IC_{50} value of 247 nM, in good agreement with its affinity for the receptor (Fig. 2B, Table 2).

3.2. Molecular modeling

3.2.1. Receptor structures

In the cases where X-ray structures of the receptors were available (dopamine D_2 and D_3 receptors, serotonin 5-HT_{2A} receptor), they were used for molecular docking as described in the Materials and Methods section. In the case of dopamine D_1 (Kaczor et al., 2016d) and serotonin 5-HT_7 (Kaczor et al., 2020) receptors, previously published homology models were used.

As D2AAK3 is an agonist of serotonin 5-HT_{1A} receptor, the model of this receptor in active conformation was constructed. The model contains a disulphide bridge between Cys109 and Cys187. The Ramachandran plot of the final homology model of the receptor is shown in Fig. 3. The plot confirms a very good quality of the constructed homology model. The only residue lying outside the allowed region is Gly105 (Gly (3.21) according to Ballesteros-Weinstein nomenclature (Ballesteros and Weinstein, 1995). However, glycine has no side chain and can adopt phi and psi angles in all four quadrants of the Ramachandran plot. A very good quality of the constructed homology model is also confirmed by its superimposition with the homology model of serotonin 5-HT_{1A} receptor in an active conformation available in GPCRdb (Pándy-Szekeres et al., 2018) built on the same template, resulting in root-mean-square deviation (RMSD) of the transmembrane region of 0.159 Å.

3.2.2. Ligand-receptor-interactions

In order to study the interactions of D2AAK3 with respective receptors, molecular docking was carried out. The binding poses of the ligand are presented in Fig. 4. It can be observed that D2AAK3 adopts a similar binding pose in all the studied receptors with indazole moiety directing towards the extracellular vesibule and 3-(trifluoromethyl)phenyl group

penetrating deeper into the binding pockets of the receptors. In case of all the receptors the main anchoring point is the electrostatic interaction between the protonatable nitrogen atom of D2AAK3 and the conserved Asp (3.32) from the third transmembrane helix. In case of dopamine D_1 and D_2 receptors the binding conformation of D2AAK3 is bent while it is more exteneded in the other molecular targets.

In case of dopamine D_1 receptor (Fig. 4A) D2AAK3 forms additional hydrogen bond between the indazole nitrogen atoms and NH group from the main chain of Ser 188 from the extracellular loop 2 (ecl2). For the dopamine D_2 receptor (Fig. 4B) an additional hydrogen bond was found between the amide oxygen atom of D2AAK3 and the main chain oxygen atom of Thr (7.38). Moreover, π-π stacking interactions occur between the D2AAK3 aromatic moieties and Trp (6.48), Phe (6.52), His (6.55) and Tyr (7.34). The obtained docking pose of D2AAK3 in dopamine D_2 receptor and the multiple interactions the ligand forms with this receptor are in accordance with the good affinity of D2AAK3 to the receptor. Regarding the dopamine D_3 receptor (Fig. 4C), D2AAK3 forms an additional hydrogen bond between the indazole NH hydrogen atom and the side chain of Glu (2.64) and forms π-π stacking interactions between its 3-(trifluoromethyl)phenyl group and Phe (6.52). In case of all receptors D2AAK3 fits well to the binding cavities as depicted in Fig. 5A-C using non-covalent interaction (NCI) maps. Non-Covalent Interactions is a visualization index derived from the density an identification of non-covalent interactions. It is based on the peaks that appear in the reduced density gradient (RDG) at low densities.

In case of serotonin 5-HT_{1A} receptor (Fig. 4D) D2AAK3 forms a hydrogen bond between its protonatable nitrogen atom and the oxygen atom from the side chain of Asn (7.38). The indazole and 3-(trifluoromethyl)phenyl groups of the ligand are involved in π-π stacking interactions with Trp (7.39) and Phe (6.52), respectively. Regarding serotonin 5-HT_{2A} receptor (Fig. 4E) the indazole NH hydrogen of D2AAK3 forms a hydrogen bond with the hydroxylic gropup of Ser (2.60). Similarly as in the case of serotonin 5-HT_{1A} receptor and most dopamine receptors 3-(trifluoromethyl)phenyl group of the ligand is engaged in π-π stacking interactions with Phe (6.52) which is in agreement with good affinity of D2AK3 to this receptor. Finally, concerning serotonin 5-HT7 receptor (Fig. 4F), the indazole NH hydrogen atom of D2AAK3 interacts via a hydrogen bond with the side chain of Asp (2.64) while its amide oxygen atom forms a hydrogen bond with the NH hydrogen atom of the main chain of of Ile 233 from ecl2. Similarly as for dopamine receptors D2AAK3 fits well to binding pockets of the serotonin receptors (Fig. 5D-F).

3.2.3. Dynamic aspects of ligand-receptor interactions

In order to study the stability of ligand-receptor complexes obtained in the molecular docking and to investigate the changes of interactions of D2AAK3 with the receptors in time, 200 ns molecular dynamics simulations were performed. The values of ligand RMSD plotted in Fig. S2 in Supplementary Information prove the correctness of the carried out molecular dynamics simulations and the stability of the systems. Aiming to describe the dynamic aspects of ligand-receptor interactions histograms (Fig. 6 and 7) and summary plots of interactions (Fig. S3 and S4 in Supplementary Information) were produced.

For all the studied receptors the interaction between the protonatable nitrogen atom of D2AAK3 and Asp (3.32) – ionic or hydrogen bond – is maintained during 100% of the simulation time. In the case of dopamine D_1 receptor (Fig. 6A and S3A) hydrogen bonds or water bridged interactions were formed by D2AAK3 with Lys 81 (2.60) for about 50% of the simulation time), Ala 84 (2.63) for about 30% of the simulation time, Gly 88 from the first extracellular loop (ecl1) for about 40% of the simulation time, Ser 310 (7.31) for about 40% of the simulation time and Asn 311 (7.32) for about 40% of the simulation time. D2AAK3 is also involved in hydrophobic interactions with Trp 99 (3.28), Leu 190 from ecl2, Phe 288 (6.51) and Phe 289 (6.52) for about 50%, 10%, 30% and 60% of the simulations time, respectively. Regarding dopamine D_2 receptor (Fig. 6B and S3B) D2AAK3 forms a hydrogen bond with Cys 182 from ecl2 for about 100% of the simulations time and water bridged/hydrophobic interactions with Leu 94 (2.63), Ile 184 from ecl2 and Tyr 408 (7.34) for about 90%, 50% and 70% of the simulations time, respectively. The ligand is also involved in hydrophobic contacts with Phe 390 (6.52) of the receptor for about 70% of the simulations time. In case of dopamine D_3 receptor (Fig. 6C and S3C) D2AAK3 is involved in hydrogen bond/hydrophobic interactions with Tyr 36 (1.39) for about 35% of the simulations time and in water bridged/hydrophobic interactions with Tyr 365 for about 50% of the simulations time. Moreover, the ligand forms hydrophobic contacts with Val 86 (2.60), Phe 345 (6.51) and Phe 346 (6.52) for about 30%, 30% and 80% of the simulations time, respectively.

Considering serotonin 5-HT_{1A} receptor (Fig. 7A and S4A) D2AAK3 is involved in water bridged interactions with Ala 93 (2.60) and Asn 386 (7.38) for about 20% and 50% of

the simulations time, respectively. Furthermore, the ligand forms hydrogen bond/water bridged interactions with Gln 97 (2.64) for about 40% of the simulations time. D2AAK3 is also engaged in water bridged/hydrophobic contacts with Tyr 96 (2.63), Leu 380 (7.32) and Ala 383 (7.35) for about 80%, 25% and 60% of the simulations time, respectively. The ligand forms hydrophobic interactions with Lys 191 from ecl2 and Phe 362 (6.52) for about 25% of the simulations time for both residues. In case of serotonin 5-HT_{2A} receptor (Fig. 7B and S4B) the ligand form water bridged interactions with Asn 343 (6.55) for about 40% of the simulations time, hydrogen bond/water bridged interactions with Asn 363 (7.35) for about 30% of the simulations time and water bridged/hydrophobic contacts with Ala 230 from ecl2 for about 30% of the simulations time. D2AAK3 is also involved in hydrophobic interactions with Val 156 (3.33) , Phe 339 (6.51) and Phe 340 (6.52) for about 40%, 30% and 20% of the simulations time, respectively. Regarding the interactions of D2AAK3 with serotonin 5-HT_7 receptor (Fig. 7C and S4C) the ligand is involved in water bridged interactions with Val 138 (2.60) and Glu 366 (7.34) for about 25% and 80% of the simulations time, respectively. It also forms hydrogen bond/water bridged contacts with Cys 231 from ecl2 for about 35% of the simulations time. The most important hydrophobic contacts of the ligand are those with Cys 166 (3.36), Phe 343 (6.51), Phe 344 (6.52), Leu 370 (7.38) and Trp 371 (7.39) which are maintained for 40%, 60%, 30%, 40% and 25% of the simulations time, respectively.

The intensive interactions of D2AAK3 with dopamine D_2 and serotonin 5-HT_{1A} receptors observed in molecular dynamics simulations correspond to the molecular docking results and good affinity of the ligand to these receptors.

3.3. Behavioral studies

3.3.1. D2AAK3 effects on motor coordination in mice

D2AAK3 at the studied doses (50 mg/kg and 100 mg/kg, i.p.) does not induce coordination impairments as evaluated in the rotarod and chimney tests. For instance, the ability of animals to keep balance on a rotating rod during 60 s (mean ± SEM) was measured for D2AAK3 (100 mg/kg) and control group (55.71 ± 2.17 and 59.14 ± 0.46, respectively). For chimney test, the ability of animal to go backwards, vertically from the tube, was assessed and the values (mean ± SEM) for D2AAK3 (100 mg/kg) and control group were 11.64 ± 0.81 and 9.86 ± 0.74, respectively.

3.3.2. Effects of D2AAK3 on spontaneous locomotor activity and amphetamine-induced hyperactivity in mice

The effect of D2AAK3 on the spontaneous locotomor activity in mice is presented in Fig. 8. Two-way ANOVA revealed that in a group of mice co-administrated with D2AAK3 (100 mg/kg, i.p.) and amphetamine (5 mg/kg, s.c.) there is a statistically significant treatment effect [$F(1,27) = 12.46$, $p = 0.0015$], statistically significant pretreatment effect [$F(1,27) = 12.82$, $p = 0.0013$], and statistically significant interaction effect between treatment and pretreatment [$F(1,27) = 6.13$, $p = 0.0198$]. Indeed, the post hoc Newman-Keuls's test showed that administration of amphetamine increased the locomotor activity of mice when compared to control group ($p < 0.001$, Fig. 8), and that D2AAK3 co-administered with amphetamine (5 mg/kg) decreased amphetamine-induced hyperactivity when compared to the amphetamine-

treated group ($p < 0.001$). However, D2AAK3 alone did not show statistically significant difference when compared with control group ($p > 0.05$).

3.3.3. Effect of acute administration of D2AAK3 on memory consolidation in mice

The D2AAK3 effect on memory consolidation was determined during the retention trial of the PA task (Fig. 9A). T-test revealed that the acute administration of D2AAK3 (100 mg/kg; i.p.) induces statistically significant increase in the IL values ($p = 0.0075$) compared to respective-vehicle treated group. More specifically, the enhancement of the memory consolidation was observed after D2AAK3 treatment.

To determine if D2AAK3 (50 mg/kg, i.p.) can reverse the MK-801-induced memory impairment mice were co-injected with the combination of D2AAK3 (50 mg/kg, i.p.) and MK-801 (0.3 mg/kg, i.p.). Two-way ANOVA revealed that there is a statistically significant D2AAK3 pretreatment effect [$F(1,47) = 16.85$, $p = 0.0002$], statistically significant MK-801 treatment effect [$F(1,47) = 6.092$, $p = 0.0173$], and no significant interaction effect between treatment and pretreatment [$F(1,47) = 0.092$, $p = 0.7630$]. However, the Newman-Keuls's post hoc test indicated the increase of IL index in mice treated with 50 mg/kg D2AAK3 and MK-801 when compared to respective MK-801-treated group ($p < 0.05$, Fig. 9B) what suggests that studied compound reverses memory impairment in mice.

3.3.4. Anxiety-like effects after D2AAK3 treatment in mice

To evaluate the influence of the acute administration of D2AAK3 on anxiety responses in male Swiss mice, EPM tests were performed. The statistical analysis (t-test) of the results for the activity of D2AAK3 (100.0 mg/kg) on anxiety responses indicated significant influence on

the percentage of the time spent in the open arms ($p < 0.0001$) (Fig. 10) and the percentage of the open arm entries ($p < 0.0001$) (Fig. 10) 30 minutes after D2AAK3 administration. In this regard, the decrease in both percentage of the time spent in the open arms and the open arm entries indicates the anxiogenic activity of D2AAK3. However, this effect was not statistically significant 60 min after D2AAK3 acute treatment ($p = 0.9978$ for percentage of the time spent in the open arms and $p = 0.7264$ for the percentage of the open arm entries) (Fig. 10).

4. Discussion

In this study we presented detailed *in silico*, *in vitro* and behavioral characterization of D2AAK3, a virtual hit identified in previously conducted virtual screening (Kaczor et al., 2016c). Such elaboration is useful in order to plan hit to lead studies and lead structure optimization towards finding analogues with more advantageous properties that, in the future, may become novel antipsychotics.

D2AAK3 may be described as a multi-target ligand, since it has high affinity for dopamine D_2 and serotonin 5-HT_{1A}, 5-HT_{2A} receptors and moderate affinity for D_1 and D_3 receptors. Antagonism towards both D_2 and 5-HT_{2A} receptors is significant when it comes to antipsychotic properties, although the optimization of D2AAK3 aimed at increasing 5-HT_{2A}/D_2 affinity ratio would allow to achieve receptor profile that to a greater extent resembles atypical antipsychotics. Importantly, D2AAK3 possesses balanced activity towards main targets of interest in the treatment of schizophrenia, namely D_2, 5-HT_{2A} and 5-HT_{1A} receptors. The difference in affinities for these targets does not exceed one order of magnitude, what is one of the determinants of well-designed multi-target drugs (Bolognesi, 2019).

D2AAK3 exhibits low affinity for serotonin 5-HT_7 receptor, which was reported to play role in treating memory impairments in schizophrenia. Thus, optimized analogues of the virtual hit would benefit from displaying higher affinity and antagonism at 5-HT_7 receptor. D2AAK3 has also low affinity for muscarinic M_1 receptor and moderate affinity for histamine H_1 receptor, which are known as off-targets in managing the symptoms of schizophrenia. Blockade of histamine H_1 receptors results in sedation and weight gain, what constitutes one of the main issues related to treatment with some of atypical antipsychotics. Further optimization of D2AAK3 should result in decreased activity towards this receptor to minimalize the risk of such side effects. Antagonism at muscarinic M_1 receptor leads to memory disturbances whereas stimulating it or positive allosteric modulation may beneficially contribute to managing cognitive impairments in schizophrenia. In this context D2AAK3, having low affinity for this receptor, may prevent from occurring cognitive disorders.

D2AAK3 exhibits multi-target profile of action, what is significant in terms of treating wide range of symptoms of schizophrenia. Such approach in drug discovery is nowadays considered more promising than single-target approach in case of complex diseases, such as cancer, schizophrenia or neurodegenerative diseases (Kondej et al., 2018b). This complexity reflects in engaging several receptors or enzymes in the pathomechanism of certain disease, thus it is more favorable to target several of them than just one. Administration of one multi-target drug instead of a bunch of selective drugs is also beneficial in terms of pharmacokinetic profile, drug-drug interactions or side effects profile.

D2AAK3 blocks both dopamine D_2 and serotonin 5-HT_{2A} receptors, what is important for its activity as a potential atypical antipsychotic. All antipsychotic drugs introduced to the clinical practice are antagonists or partial/biased agonists of dopamine D_2 receptor. Such activity benefits in treating positive symptoms of schizophrenia. However, antagonism towards this receptor in other brain regions is responsible for occurrence of wide range of side effects, mainly extrapyramidal side effects and hyperprolactinemia. Combined antagonism to dopamine D_2 receptor and serotonin 5-HT_{2A} receptor of D2AAK3 may contribute to reducing those side effects arising from striatal dopamine dysregulation (Amato et al., 2018). Moreover, blocking serotonin 5-HT_{2A} receptor may lead to reducing negative and cognitive symptoms of the disease by increasing the release of dopamine in prefrontal cortex (Di Sciascio and Riva, 2015).

Balance between agonism at 5-HT_{1A} receptor and antagonism or partial agonism at D_2 receptor may result in more effective management of broader spectrum of schizophrenia symptoms, including cognitive impairment, anxiety and depressive episodes, and improve drug tolerance (Di Sciascio and Riva, 2015). Furthermore, 5-HT_{1A} receptor agonists increase the level of prefrontal dopamine, what is assumed to improve negative symptoms of schizophrenia. Besides alleviating cognitive, negative and affective disorders, targeting 5-HT_{1A} receptor seems to reduce extrapyramidal side effects induced by antipsychotics. In view of the above, D2AAK3 has the potential to reduce all types of the symptoms of schizophrenia, as it maintains that balance, being high affinity agonist for 5-HT_{1A} receptor and possessing relatively high affinity for D_2 receptor.

In vitro studies of D2AAK3 were complemented with molecular modeling investigations. The model of serotonin 5-HT_{1A} receptor in an active conformation constructed using cryo-EM structure of serotonin 5-HT_{1B} receptor in complex with an agonist donitriptan as a template is reported here. The model is very close to the model from GPCRdb constructed based on the same template (RMSD of transmembrane region of 0.159 Å) which confirms its very good quality. The model is also in general agreement with previously published models of this receptor in active conformation which were built using other templates (see eg. (Del Bello et al., 2017)). The obtained docking poses of D2AAK3 in the studied aminergic GPCRs with the electrostatic interaction between the protonatable nitrogen atom of the ligand and Asp (3.32) follow the general pharmacophore model for aminergic GPCRs ligands and resulting ligand-receptor interactions mode (Kaczor et al., 2016b). In most receptors D2AAK3 also interacts with Phe (6.52) which is in agreement with our earlier studies on D2AAK1 (Kaczor et al., 2016d) and its derivatives (Kondej et al., 2019, 2018a). The position of D2AAK3 in the binding pocket with the indazole moiety directing towards the extracellular vestibule is also in accordance with the results for D2AAK1 (Kaczor et al., 2016d) and its derivatives (Kondej et al., 2019, 2018a) where indole group was directed to the exterior of the receptor. A similar binding pose was found for ritanserin in X-ray structure of its complex with serotonin 5-HT_{2C} receptor (Peng et al., 2018). A good fit of D2AAK3 to the binding pockets of the studied proteins was additionally confirmed using non-covalent interaction maps. The obtained ligand-receptor complexes were stable in 200 ns molecular dynamics simulations. The mode of D2AAK3-receptors interactions in molecular dynamics simulations followed the one from

molecular docking (interactions with Asp (3.32), Phe (6.51) and Phe (6.52)) and corresponded to the affinity of D2AAK3 to different receptors.

Behavioral studies confirmed antipsychotic activity of D2AAK3 expected based on *in vitro* tests results. The compound decreases the hyperactivity induced by the administration of amphetamine in mice at studied dose of 100 mg/kg.

The impact of D2AAK3 acute administration on memory processes was evaluated in the PA task. Our results indicated that the studied compound (100 mg/kg) improves memory processes in mice. Moreover, D2AAK3, in a lower dose (50 mg/kg) reverses MK-801-induced memory impairments in mice. Cognitive symptoms associated with schizophrenia generally remain resistant to the treatment with available antipsychotics. Furthermore, it was reported that some antipsychotics, such as clozapine, olanzapine or asenapine, not only fail in reducing memory-associated symptoms of schizophrenia, but even impair the PA task performance in rodents (Kołaczkowski et al., 2014). In case of first generation antipsychotics, it has been shown that haloperidol impaired the spatial learning memory in Morris water maze (MWM) in mice (Xu et al., 2012). In addition, haloperidol and olanzapine disturbed cognitive function in MWM test in mice (Mutlu et al., 2011). However, in the PA test, haloperidol did not affect memory-related responses when was administered before the training or retention test (Ichihara et al., 1988). In addition, olanzapine but not haloperidol reversed MK-801-induced memory impairments in mice using the MWM test (Song et al., 2016). Similarly, risperidone also reversed MK-801-induced impairments in rats using the modified elevated plus maze test (Celikyurt et al., 2011), probably due to its antagonistic-like properties on 5-HT_{2A} receptors.

A variety of more recent studies, especially those where schizophrenia patients were followed over more extended periods of time, do not support the view that antipsychotics (in general) significantly improve cognition in schizophrenia (Nielsen et al., 2015). In particular, clozapine compared to other antipsychotics, was not superior in the cognitive function and may even be associated with decreased working memory performance. In a recent study, Czepielewski et al. (Czepielewski et al., 2018) compared treatment-resistant subjects with schizophrenia under long term clozapine treatment with cases using other antipsychotics who never used clozapine, and showed that clozapine did not improve verbal learning ability better than other antipsychotics. However, individual differences in clozapine's effect on short term episodic memory may be associated with plasma level of clozapine, N-desmethylclozapine (major metabolite of clozapine) and polymorphism in the M_1-cholinergic receptors as well (Kır et al., 2020).

Hence, there is still a need to develop antipsychotics capable of managing cognitive impairments in schizophrenia. The memory consolidation is referring to the process by which a temporary, labile memory is transformed into a more stable, long-lasting form that has been shown to be most specifically disrupted in schizophrenic patients (Baran et al., 2018; Wamsley et al., 2012). Moreover, concerning the molecular events underlying consolidation, an involvement of D_1 and D_2 receptors modulation has been revealed.

In order to evaluate the influence of D2AAK3 on anxiety-like behavior, EPM test was conducted. The compound turned out to elicit anxiety-like responses 30 min after acute treatment. However, this effect has not been observed 60 min after D2AAK3 administration –

lack of statistically significant differences between drug-treated and control group (in both % open arms entries and % open arm time). This dual effect may be associated with the affinity of D2AAK3 for serotonin 5-HT_{1A} receptor. The serotonin system in the brain is known to be involved in anxiety and mood regulation – many commonly prescribed anxiolytics and antidepressants act via targeting this system. Regarding anxiety, attention has been paid particularly to the 5-HT_{1A} receptor (Heisler et al., 1998). Buspirone, commonly prescribed anxiolytic agent is an agonist of 5-HT_{1A} autoreceptor, that if activated leads to the neuronal suppression within serotonergic system and thus elicit anxiolytic effect (Balaj et al., 2019). Also 8-hydroxy-2-(di-n-propylamino)tetralin (8-OH-DPAT), the tool compound to study 5-HT_{1A} receptor and its highly selective agonist, exerts multiple pharmacological effects, among others anxiolytic effect. However, activation of another population of 5-HT_{1A} receptors, located postsynaptically in brain structures such as amygdala, dorsal hippocampus and cerebral cortex, is reported to produce anxiety-like responses (Heisler et al., 1998). After direct administration of 8-OH-DPAT to the dorsal hippocampus, significant anxiogenic effect was observed in the plus maze and in the social interaction test (File et al., 1996). Taking the above into account, we may presume that the effect of D2AAK3 on anxiety-related responses arises from affecting signaling via 5-HT_{1A} receptor, as the compound is its high affinity full agonist. Hypothetically, the initial anxiogenic effect observed 30 min after D2AAK3 administration may emerge from activation of postsynaptic 5-HT_{1A} receptors in dorsal hippocampus, yet being not observed 60 min after acute treatment due to stimulating 5-HT_{1A} autoreceptors and thus decreasing the release of serotonin in nerve terminals in the limbic system.

In case of other antipsychotics, it has been shown that risperidone decreased anxiety levels in the open field and elevated plus maze (EPM) tests (Karl et al., 2006). Similarly, haloperidol presented anxiolytic activity in mice by inducing the increase in percentage of the open arm time and percentage of the open arm entries in EPM test (Ulak et al., 2016). It has also been reported that acute but not chronic treatment with olanzapine induces anxiolytic activity only in stressed rats (Locchi et al., 2008).

5. Conclusions

As a result of the virtual screening aimed at searching for potential novel antipsychotics, virtual hit D2AAK3 was found, and afterwards subjected to *in silico*, *in vitro* and behavioral studies in order to evaluate its activity. Revealed beneficial pharmacological properties along with balanced multi-target profile of the compound indicate that optimization of D2AAK3 may result in obtaining derivatives that will be further considered as a promising lead molecule for novel antipsychotics.

Author statement:

Conceptualization, A.A.K..; methodology, A.A.K., K.T.-D. and M.C.; investigation, A.A.K., K.T.-D., A.G.S., M.K.-S. and M.C.; resources, A.A.K.; writing—original draft preparation, A.A.K., K.T.-D., P.S., and M.C.; writing—review and editing, A.A.K., K.T.-D., P.S., A.G.S., O.K., E.K., A.G., M.K.-S., G.B. and M.C.; visualization, A.A.K., K.T.-D. and M.C.; supervision, A.A.K. and M.C.; project administration, A.A.K.; funding acquisition, A.A.K. and M.C.. All authors have read and agreed to the published version of the manuscript

Funding:

The research was performed under OPUS grant from National Science Center (NCN, Poland), grant number 2017/27/B/NZ7/01767 (to A.A.K.). Calculations were partially performed under a computational grant by Interdisciplinary Center for Mathematical and Computational Modeling (ICM), Warsaw, Poland, grant number G30-18, under resources and licenses from CSC, Finland.). In vitro pharmacology assays were performed with support from the Spanish Ministry of Economy and Competitiveness (MINECO) (grant number SAF2014-57138-C2-1-R to M.C.). A.G.S. acknowledges funding from XUNTA de Galicia (Spain).

Conflicts of Interest:

The authors declare no conflict of interest. The funders had no role in the design of the study; in the collection, analyses, or interpretation of data; in the writing of the manuscript, or in the decision to publish the results.

Figure captions:

Fig. 1. Structural formula of D2AAK3.

Fig. 2. Functional assays for D2AAK3 at 5-HT_{1A} and 5-HT_{2A} receptors. (A) Concentration-response curves of D2AAK3 and 5-CT (as reference agonist) at inhibiting forskolin-stimulated cAMP production in HEK293 cells expressing human cloned 5-HT_{1A} receptors. The graph shows data (mean ± SEM) of three independent experiments performed in triplicate. (B) Concentration-response curves of D2AAK3 and risperidone (as reference antagonist) on IP production stimulated by 1 μM 5-HT in CHO-K1 cells expressing human cloned 5-HT_{2A}

receptors. The graph shows data (mean ± SEM) of two independent experiments performed in duplicate.

Fig. 3. The Ramachandran plot of the homology model of serotonin 5-HT_{1A} receptor. Most residues are represented by circles. Glycines are depicted as triangles while prolines as squares. The only residue lying outside the allowed region is Gly 105 (Gly (3.21)). However, glycine has no side chain and can adopt phi and psi angles in all four quadrants of the Ramachandran plot.

Fig. 4. D2AAK3 in complex with dopamine D_1 (A), D_2 (B), D_3 (C) and serotonin 5-HT_{1A} (D), 5-HT_{2A} (E) and 5-HT_7 receptors. Proteins shown in wire representation with cyan carbon atoms. The most important residues shown as sticks. Ligand shown as sticks with grey carbon atoms. Polar interactions represented as red dashed lines. Non-polar hydrogen atoms omitted for clarity.

Fig. 5. Non-covalent interactions maps for D2AAK3 in complex with dopamine D_1 (A), D_2 (B), D_3 (C) and serotonin 5-HT_{1A} (D), 5-HT_{2A} (E) and 5-HT_7 receptors. Weak attractive interactions shown in green. Proteins shown in iceblue as cartoon representation. Asp 3.32 shown in yellow in stick representation. D2AAK3 shown in CPK representation with cyan carbon atoms.

Fig. 6. Histograms of the molecular interactions of D2AAK3 with human dopamine D_1 (A), D_2 (B) and D_3 (C) receptor during molecular dynamics simulations (200 ns). The stacked bar charts are normalized over the course of the trajectory: for example, a value of 0.7 suggests that the specific interaction is maintained during 70% of the simulation. Values over 1.0 indicate that some protein residue may maintain multiple contacts with the ligand.

Fig. 7. Histograms of the molecular interactions of D2AAK3 with human serotonin 5-HT_{1A} (A), 5-HT_{2A} (B) and 5-HT_{7} receptor during molecular dynamics simulations (200 ns). The stacked bar charts are normalized over the course of the trajectory: for example, a value of 0.7 suggests that the specific interaction is maintained during 70% of the simulation. Values over 1.0 indicate that some protein residue may maintain multiple contacts with the ligand.

Fig. 8. The influence of an acute injection of D2AAK3 on the amphetamine-induced hyperactivity in mice. Appropriate groups of mice received D2AAK3 [(100 mg/kg; i.p. (n = 7)], amphetamine [5 mg/kg, (n = 8); s.c.], 100 mg/kg D2AAK3 co-injected with 5 mg/kg amphetamine (n = 8), and vehicle (n = 8, indicated as 0). Data are shown as the distance traveled (cm) by mouse recorded for 30 min (mean ± SEM). The results from the Tukey's test analyses presented: ***$p < 0.01$ amphetamine vs. the vehicle-treated group and ^^^$p < 0.001$ 100 mg/kg D2AAK3 vs. amphetamine-treated group.

Fig. 9. Acute effect of D2AAK3 on memory consolidation (A) and D2AAK3 effect on MK-801-induced memory impairment (B) in mice assessed in passive avoidance (PA) test. Appropriate mice groups received acute injections of D2AAK3 [50 and 100 mg/kg (n = 8-13), vehicle (n = 9-13, indicated as 0), D2AAK3 (50 mg/kg) + MK-801 (n =13) and MK-801 alone (n = 12); i.p.] on Day 1 immediately after the PA test. Then, these rodents were retested on Day 2 (i.e., 24 h later) as reported previously (Kaczor et al., 2016d). Data are presented as mean ± SEM. For the panel A: the results from the t-test analyses indicate: **$p = 0.0075$ when compared with the control group. For the panel B: the results from the post hoc Newman-

Keuls's test indicated: *p < 0.05 for D2AAK3+MK-801 when compered to MK-801-treated group; ^^^p < 0.001 D2AAK3 vs control group and #p < 0.05 for MK-801 vs control group.

Fig. 10. Acute effect of D2AAK3 on anxiety-like responses in mice evaluated 30 and 60 minutes after treatment using elevated plus maze (EPM) test. Percentage (%) of open arm entries (A and C) and % of time spent in the open arms (B and D) recorded 30 (A and B) and 60 (C and D) minutes after 100 mg/kg D2AAK3 injection [(n = 8) and vehicle (n = 8, indicated as 0); i.p). Data are presented as mean ± SEM. The t-test analyses indicated the anxiogenic activity elicited by D2AAK3 30 minutes after treatment *** p < 0.001 for time spent in the open arms and open arm entries but not statistically significant after 60 minutes.

Tables:

Table 1. Experimental radioligand binding data for D2AAK3.

Table 2. Evaluation of potency and efficacy of compound D2AAK3 at the indicated receptors in *in vitro* functional assays.

References

Amato, D., Canneva, F., Cumming, P., Maschauer, S., Groos, D., Dahlmanns, J.K., Grömer, T.W., Chiofalo, L., Dahlmanns, M., Zheng, F., Kornhuber, J., Prante, O., Alzheimer, C., von Hörsten, S., Müller, C.P., 2018. A dopaminergic mechanism of antipsychotic drug efficacy, failure, and failure reversal: the role of the dopamine transporter. Mol. Psychiatry 1–18. https://doi.org/10.1038/s41380-018-0114-5

Balaj, K., Nowinski, L., Walsh, B., Mullett, J., Palumbo, M.L., Thibert, R.L., McDougle, C.J., Keary, C.J., 2019. Buspirone for the treatment of anxiety-related symptoms in Angelman syndrome: a case series. Psychiatr Genet 29, 51–56. https://doi.org/10.1097/YPG.0000000000000218

Ballesteros, J. A., Weinstein, H., 1995. Integrated methods for the construction of three-dimensional models and computational probing of structure-function relations in G protein-coupled receptors. Methods Neurosci. 25, 366–428, DOI: 10.1016/S1043-9471(05)80049-7.

Baran, B., Correll, D., Vuper, T.C., Morgan, A., Durrant, S.J., Manoach, D.S., Stickgold, R., 2018. Spared and impaired sleep-dependent memory consolidation in schizophrenia. Schizophr. Res. 199, 83–89. https://doi.org/10.1016/j.schres.2018.04.019

Barnes, T.R., Drake, R., Paton, C., Cooper, S.J., Deakin, B., Ferrier, I.N., Gregory, C.J., Haddad, P.M., Howes, O.D., Jones, I., Joyce, E.M., Lewis, S., Lingford-Hughes, A., MacCabe, J.H., Owens, D.C., Patel, M.X., Sinclair, J.M., Stone, J.M., Talbot, P.S., Upthegrove, R., Wieck, A., Yung, A.R., 2020. Evidence-based guidelines for the pharmacological treatment of schizophrenia: Updated recommendations from the British Association for Psychopharmacology. J. Psychopharmacol. (Oxford) 34, 3–78. https://doi.org/10.1177/0269881119889296

Bolognesi, M.L., 2019. Harnessing Polypharmacology with Medicinal Chemistry. ACS Med. Chem. Lett. 10, 273–275. https://doi.org/10.1021/acsmedchemlett.9b00039

Bowers, Bowers, K. J., Chow, E., Xu, H., Dror, R. O., Eastwood, M. P., Gregersen, B. A., Klepeis, J. I., Kolossváry, I., Moraes, M. A., Sacerdoti, F. A., Salmon, J. K., Shan, Y., Shaw, D. E., 2006. Scalable Algorithms for Molecular Dynamics Simulations on Commodity Clusters, Proceedings of the ACM/IEEE Conference on Supercomputing (SC06), Tampa, Florida, November 11–17, 2006.

Celikyurt, I.K., Akar, F.Y., Ulak, G., Mutlu, O., Erden, F., 2011. Effects of risperidone on learning and memory in naive and MK-801-treated rats. Pharmacology 87, 187–194. https://doi.org/10.1159/000324523

Chien, E.Y.T., Liu, W., Zhao, Q., Katritch, V., Han, G.W., Hanson, M.A., Shi, L., Newman, A.H., Javitch, J.A., Cherezov, V., Stevens, R.C., 2010. Structure of the human dopamine D3 receptor in complex with a D2/D3 selective antagonist. Science 330, 1091–1095. https://doi.org/10.1126/science.1197410

Contreras-García, J., Johnson, E.R., Keinan, S., Chaudret, R., Piquemal, J.-P., Beratan, D.N., Yang, W., 2011. NCIPLOT: a program for plotting non-covalent interaction regions. J. Chem. Theory Comput. 7, 625–632. https://doi.org/10.1021/ct100641a

Czepielewski, L.S., Londero, M.D.B., de Sousa, M.H., Perin, C.P., Maldonado, H.C., Claudino, F.C.A., Gama, C.S., 2018. Long-term treatment with clozapine and verbal memory performance in schizophrenia. Schizophr. Res Cogn. 12, 40–41. https://doi.org/10.1016/j.scog.2018.02.002

Del Bello, F., Bonifazi, A., Giannella, M., Giorgioni, G., Piergentili, A., Petrelli, R., Cifani, C., Micioni Di Bonaventura, M.V., Keck, T.M., Mazzolari, A., Vistoli, G., Cilia, A., Poggesi, E., Matucci, R., Quaglia, W., 2017. The replacement of the 2-methoxy substituent of N-((6,6-diphenyl-1,4-dioxan-2-yl)methyl)-2-(2-methoxyphenoxy)ethan-1-amine improves the selectivity for 5-HT1A receptor over α1-adrenoceptor and D2-like receptor subtypes. Eur. J. Med. Chem. 125, 233–244. https://doi.org/10.1016/j.ejmech.2016.09.026

Di Sciascio, G., Riva, M.A., 2015. Aripiprazole: from pharmacological profile to clinical use. Neuropsychiatr. Dis. Treat. 11, 2635–2647. https://doi.org/10.2147/NDT.S88117

Edgar, R.C., 2004. MUSCLE: multiple sequence alignment with high accuracy and high throughput. Nucleic Acids Res. 32, 1792–1797. https://doi.org/10.1093/nar/gkh340

File, S.E., Gonzalez, L.E., Andrews, N., 1996. Comparative study of pre- and postsynaptic 5-HT1A receptor modulation of anxiety in two ethological animal tests. J. Neurosci. 16, 4810–4815.

García-Nafría, J., Nehmé, R., Edwards, P.C., Tate, C.G., 2018. Cryo-EM structure of the serotonin 5-HT1B receptor coupled to heterotrimeric Go. Nature 558, 620–623. https://doi.org/10.1038/s41586-018-0241-9

GBD 2017 Disease and Injury Incidence and Prevalence Collaborators, 2018. Global, regional, and national incidence, prevalence, and years lived with disability for 354 diseases and injuries

for 195 countries and territories, 1990-2017: a systematic analysis for the Global Burden of Disease Study 2017. Lancet 392, 1789–1858. https://doi.org/10.1016/S0140-6736(18)32279-7

Heisler, L.K., Chu, H.-M., Brennan, T.J., Danao, J.A., Bajwa, P., Parsons, L.H., Tecott, L.H., 1998. Elevated anxiety and antidepressant-like responses in serotonin 5-HT1A receptor mutant mice. Proc. Natl. Acad. Sci. U. S. A. 95, 15049–15054.

Humphrey, W., Dalke, A., Schulten, K., 1996. VMD: Visual molecular dynamics. J. Mol. Graph.14, 33–38. https://doi.org/10.1016/0263-7855(96)00018-5

Ichihara, K., Nabeshima, T., Kameyama, T., 1988. Effects of haloperidol, sulpiride and SCH 23390 on passive avoidance learning in mice. Eur. J. Pharmacol. 151, 435–442. https://doi.org/10.1016/0014-2999(88)90540-7

Kaczor, A.A., Jörg, M., Capuano, B., 2016a. The dopamine D2 receptor dimer and its interaction with homobivalent antagonists: homology modeling, docking and molecular dynamics. J. Mol. Model. 22. https://doi.org/10.1007/s00894-016-3065-2

Kaczor, A.A., Rutkowska, E., Bartuzi, D., Targowska-Duda, K.M., Matosiuk, D., Selent, J., 2016b. Computational methods for studying G protein-coupled receptors (GPCRs). Methods Cell Biol. 132, 359–399. https://doi.org/10.1016/bs.mcb.2015.11.002

Kaczor, A.A., Silva, A.G., Loza, M.I., Kolb, P., Castro, M., Poso, A., 2016c. Structure-Based Virtual Screening for Dopamine D2 Receptor Ligands as Potential Antipsychotics. ChemMedChem 11, 718–729. https://doi.org/10.1002/cmdc.201500599

Kaczor, A.A., Targowska-Duda, K.M., Budzyńska, B., Biała, G., Silva, A.G., Castro, M., 2016d. In vitro, molecular modeling and behavioral studies of 3-{[4-(5-methoxy-1H-indol-3-yl)-1,2,3,6-tetrahydropyridin-1-yl]methyl}-1,2-dihydroquinolin-2-one (D2AAK1) as a potential antipsychotic. Neurochem. Int. 96, 84–99. https://doi.org/10.1016/j.neuint.2016.03.003

Kaczor, A.A., Targowska-Duda, K.M., Silva, A.G., Kondej, M., Biała, G., Castro, M., 2020. N-(2-Hydroxyphenyl)-1-[3-(2-oxo-2,3-dihydro-1H- benzimidazol-1-yl)propyl]piperidine-4-Carboxamide (D2AAK4), a Multi-Target Ligand of Aminergic GPCRs, as a Potential Antipsychotic. Biomolecules 10, 349. https://doi.org/10.3390/biom10020349

Karl, T., Duffy, L., O'brien, E., Matsumoto, I., Dedova, I., 2006. Behavioural effects of chronic haloperidol and risperidone treatment in rats. Behav. Brain Res. 171, 286–294. https://doi.org/10.1016/j.bbr.2006.04.004

Kenakin, T.P., 2014. A Pharmacology Primer: Techniques for More Effective and Strategic Drug Discovery, Fourth Ed. ed. Academic Press, San Diego, CA.

Kimura, K.T., Asada, H., Inoue, A., Kadji, F.M.N., Im, D., Mori, C., Arakawa, T., Hirata, K., Nomura, Y., Nomura, N., Aoki, J., Iwata, S., Shimamura, T., 2019. Structures of the 5-HT2A receptor in complex with the antipsychotics risperidone and zotepine. Nat. Struct. Mol. Biol. 26, 121–128. https://doi.org/10.1038/s41594-018-0180-z

Kır, Y., Baskak, B., Kuşman, A., Sayar-Akaslan, D., Özdemir, F., Sedes-Baskak, N., Süzen, H.S., Baran, Z., 2020. The relationship between plasma levels of clozapine and N-desmethyclozapine as well as M1 receptor polymorphism with cognitive functioning and associated cortical activity in schizophrenia. Psychiatry Res. Neuroimaging 303, 111128. https://doi.org/10.1016/j.pscychresns.2020.111128

Kołaczkowski, M., Mierzejewski, P., Bienkowski, P., Wesołowska, A., Newman-Tancredi, A., 2014. Antipsychotic, antidepressant, and cognitive-impairment properties of antipsychotics: rat profile and implications for behavioral and psychological symptoms of dementia. Naunyn Schmiedebergs Arch. Pharmacol. 387, 545–557. https://doi.org/10.1007/s00210-014-0966-4

Kondej, M., Bartyzel, A., Pitucha, M., Wróbel, T.M., Silva, A.G., Matosiuk, D., Castro, M., Kaczor, A.A., 2018a. Synthesis, Structural and Thermal Studies of 3-(1-Benzyl-1,2,3,6-tetrahydropyridin-4-yl)-5-ethoxy-1H-indole (D2AAK1_3) as Dopamine D_2 Receptor Ligand. Molecules 23, 2249. https://doi.org/10.3390/molecules23092249

Kondej, M., Stępnicki, P., Kaczor, A.A., 2018b. Multi-Target Approach for Drug Discovery against Schizophrenia. Int. J. Mol. Sci. 19, 3105. https://doi.org/10.3390/ijms19103105

Kondej, M., Wróbel, T.M., Silva, A.G., Stępnicki, P., Koszła, O., Kędzierska, E., Bartyzel, A., Biała, G., Matosiuk, D., Loza, M.I., Castro, M., Kaczor, A.A., 2019. Synthesis, pharmacological and structural studies of 5-substituted-3-(1-arylmethyl-1,2,3,6-tetrahydropyridin-4-yl)-1H-indoles as multi-target ligands of aminergic GPCRs. Eur. J. Med. Chem. 180, 673–689. https://doi.org/10.1016/j.ejmech.2019.07.050

Kruk-Slomka, M., Biala, G., 2016. CB1 receptors in the formation of the different phases of memory-related processes in the inhibitory avoidance test in mice. Behav. Brain Res. 301, 84–95. https://doi.org/10.1016/j.bbr.2015.12.023

Locchi, F., Dall'olio, R., Gandolfi, O., Rimondini, R., 2008. Olanzapine counteracts stress-induced anxiety-like behavior in rats. Neurosci. Lett. 438, 146–149. https://doi.org/10.1016/j.neulet.2008.04.017

Mutlu, O., Ulak, G., Celikyurt, I.K., Akar, F.Y., Erden, F., 2011. Effects of olanzapine, sertindole and clozapine on learning and memory in the Morris water maze test in naive and MK-801-treated mice. Pharmacol. Biochem. Behav. 98, 398–404. https://doi.org/10.1016/j.pbb.2011.02.009

Nielsen, R.E., Levander, S., Kjaersdam Telléus, G., Jensen, S.O.W., Østergaard Christensen, T., Leucht, S., 2015. Second-generation antipsychotic effect on cognition in patients with schizophrenia--a meta-analysis of randomized clinical trials. Acta Psychiatr. Scand. 131, 185–196. https://doi.org/10.1111/acps.12374

O'Callaghan, E., Turner, N., Renwick, L., Jackson, D., Sutton, M., Foley, S.D., McWilliams, S., Behan, C., Fetherstone, A., Kinsella, A., 2010. First episode psychosis and the trail to secondary care: help-seeking and health-system delays. Soc. Psychiatry Psychiatr. Epidemiol. 45, 381–391. https://doi.org/10.1007/s00127-009-0081-x

Pándy-Szekeres, G., Munk, C., Tsonkov, T.M., Mordalski, S., Harpsøe, K., Hauser, A.S., Bojarski, A.J., Gloriam, D.E., 2018. GPCRdb in 2018: adding GPCR structure models and ligands. Nucleic Acids Res. 46, D440–D446. https://doi.org/10.1093/nar/gkx1109

Peng, Y., McCorvy, J.D., Harpsøe, K., Lansu, K., Yuan, S., Popov, P., Qu, L., Pu, M., Che, T., Nikolajsen, L.F., Huang, X.-P., Wu, Y., Shen, L., Bjørn-Yoshimoto, W.E., Ding, K., Wacker, D., Han, G.W., Cheng, J., Katritch, V., Jensen, A.A., Hanson, M.A., Zhao, S., Gloriam, D.E., Roth, B.L., Stevens, R.C., Liu, Z.-J., 2018. 5-HT2C Receptor Structures Reveal the Structural Basis of GPCR Polypharmacology. Cell 172, 719-730.e14. https://doi.org/10.1016/j.cell.2018.01.001

Song, J.C., Seo, M.K., Park, S.W., Lee, J.G., Kim, Y.H., 2016. Differential Effects of Olanzapine and Haloperidol on MK-801-induced Memory Impairment in Mice. Clin. Psychopharmacol. Neurosci. 14, 279–285. https://doi.org/10.9758/cpn.2016.14.3.279

Stahl, S.M., 2001. Dopamine system stabilizers, aripiprazole, and the next generation of antipsychotics, part 1, “Goldilocks” actions at dopamine receptors. J. Clin. Psychiatry 62, 841–842. https://doi.org/10.4088/jcp.v62n1101

Stępnicki, P., Kondej, M., Kaczor, A.A., 2018. Current Concepts and Treatments of Schizophrenia. Molecules 23, 2087. https://doi.org/10.3390/molecules23082087

Ulak, G., Gumuslu, E., Mutlu, O., Ertan, M., Celikyurt, I.K., Akar, F., Erden, F., 2016. PM434. Haloperidol exerts depression-like behaviour in the forced swimming test while it has

anxiolytic-like and analgesic effects in the elevated plus maze and hot plate tests: Altered gen expression levels of FGF2, synapsin and NGF in the hippocampus of mice. Int. J. Neuropsychopharmacol. 19, 58. https://doi.org/10.1093/ijnp/pyw041.434

Varin, T., Gutiérrez-de-Terán, H., Castro, M., Brea, J., Fabis, F., Dauphin, F., Aqvist, J., Lepailleur, A., Perez, P., Burgueño, J., Vela, J.M., Loza, M.I., Rodrigo, J., 2010. Phe369(7.38) at human 5-HT(7) receptors confers interspecies selectivity to antagonists and partial agonists. Br. J. Pharmacol. 159, 1069–1081. https://doi.org/10.1111/j.1476-5381.2009.00481.x

Wamsley, E.J., Tucker, M.A., Shinn, A.K., Ono, K.E., McKinley, S.K., Ely, A.V., Goff, D.C., Stickgold, R., Manoach, D.S., 2012. Reduced sleep spindles and spindle coherence in schizophrenia: mechanisms of impaired memory consolidation? Biol Psychiatry 71, 154–161. https://doi.org/10.1016/j.biopsych.2011.08.008

Wang, S., Che, T., Levit, A., Shoichet, B.K., Wacker, D., Roth, B.L., 2018. Structure of the D2 dopamine receptor bound to the atypical antipsychotic drug risperidone. Nature 555, 269–273. https://doi.org/10.1038/nature25758

Webb, B., Sali, A., 2016. Comparative Protein Structure Modeling Using Modeller. Current Protocols in Bioinformatics 54, John Wiley & Sons, Inc., 5.6.1-5.6.37.

Xu, H., Yang, H.-J., Rose, G.M., 2012. Chronic haloperidol-induced spatial memory deficits accompany the upregulation of D(1) and D(2) receptors in the caudate putamen of C57BL/6 mouse. Life Sci. 91, 322–328. https://doi.org/10.1016/j.lfs.2012.07.025

Fig. 1.

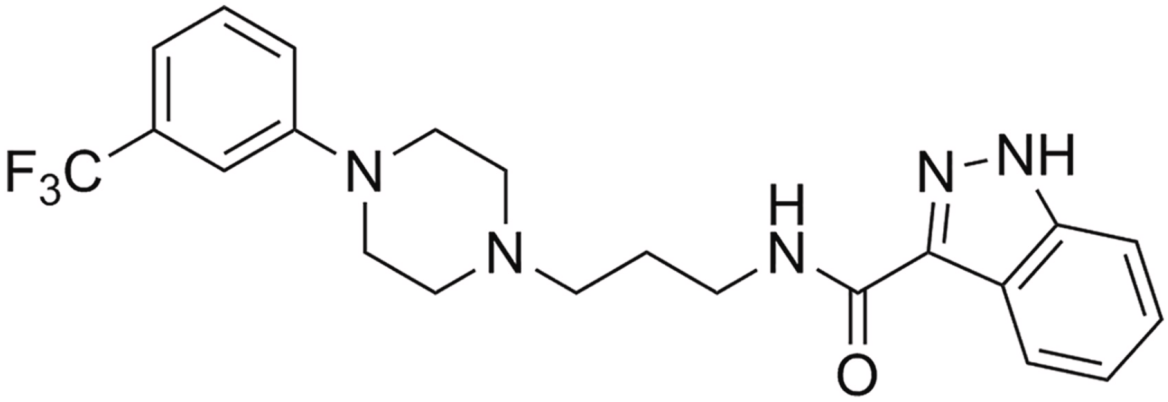

Fig. 2.

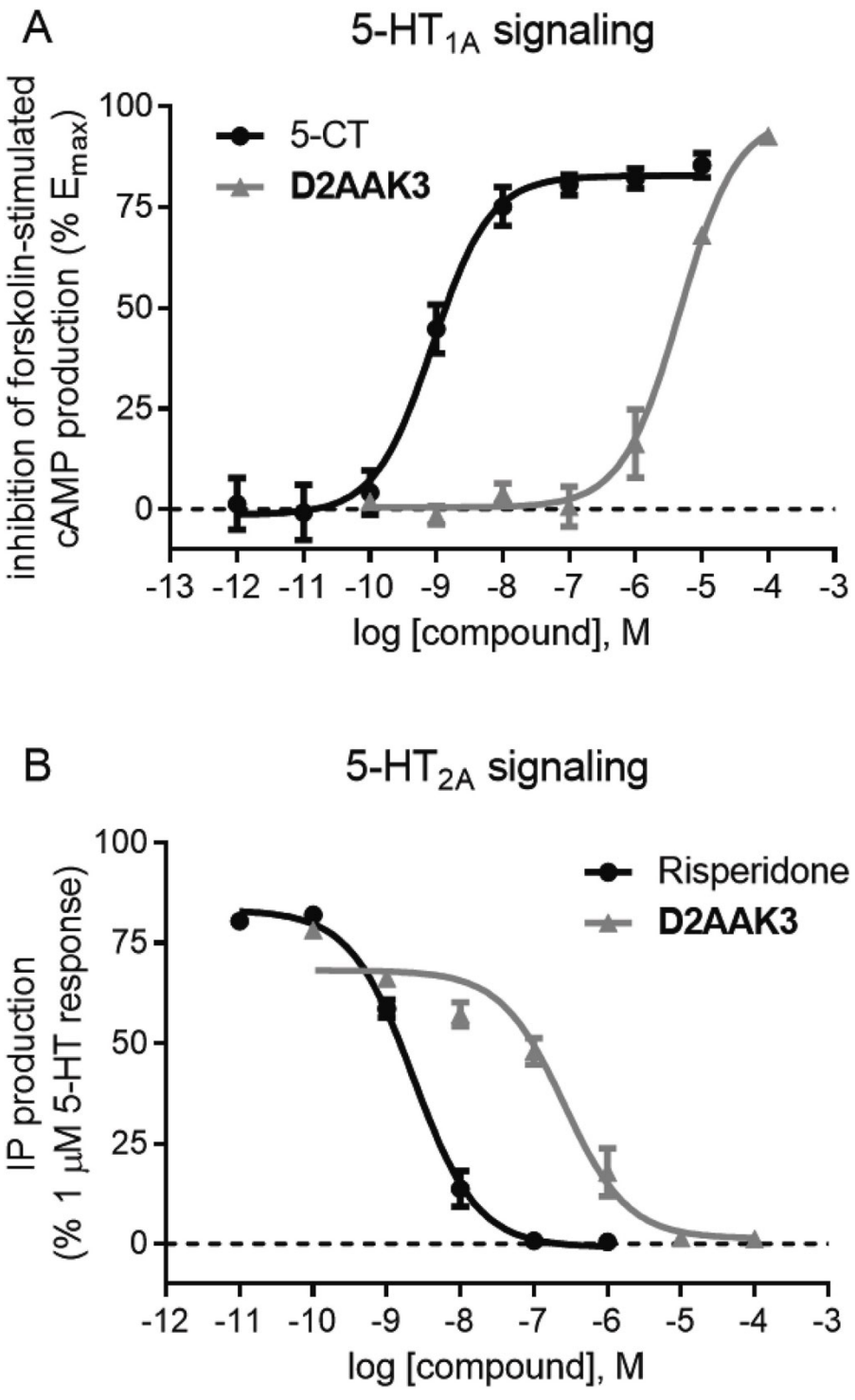
A
5-HT1A signaling
inhibition of forskolin-stimulated cAMP production (% Emax)
100
75
50
25
0
5-CT
D2AAK3
-13 -12 -11 -10 -9 -8 -7 -6 -5 -4 -3
log [compound], M
B
5-HT2A signaling
IP production (% 1 μM 5-HT response)
100
75
50
25
0
Risperidone
D2AAK3
-12 -11 -10 -9 -8 -7 -6 -5 -4 -3
log [compound], M

Fig. 3.

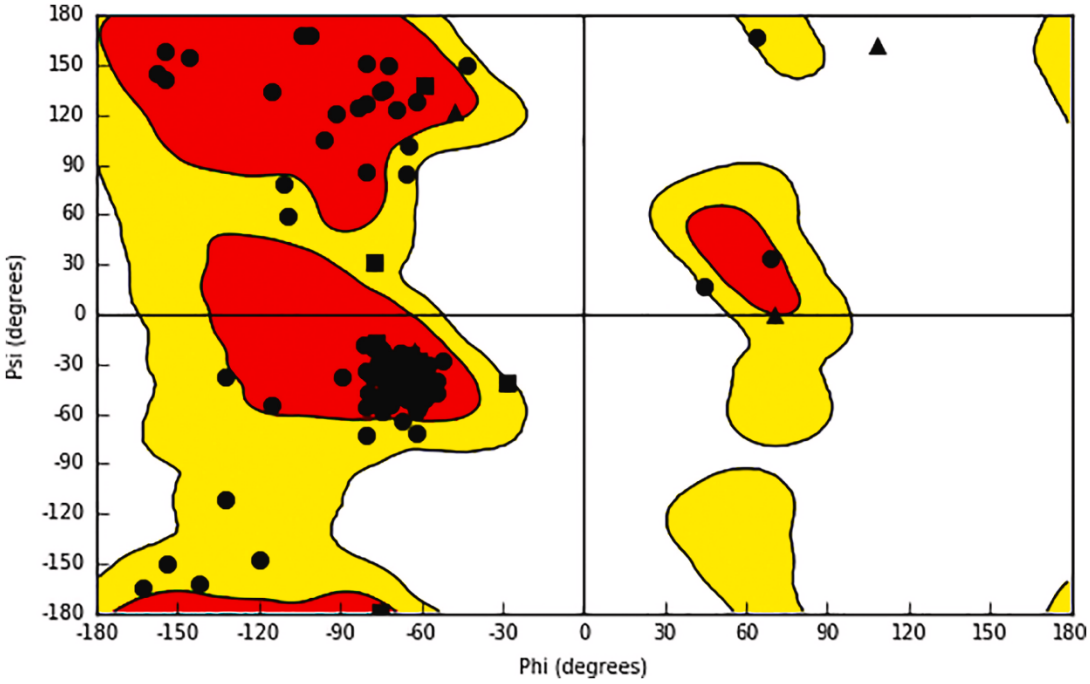
Psi (degrees)
Phi (degrees)
180
150
120
90
60
30
0
-30
-60
-90
-120
-150
-180
-180
-150
-120
-90
-60
-30
0
30
60
90
120
150
180

Fig. 4.

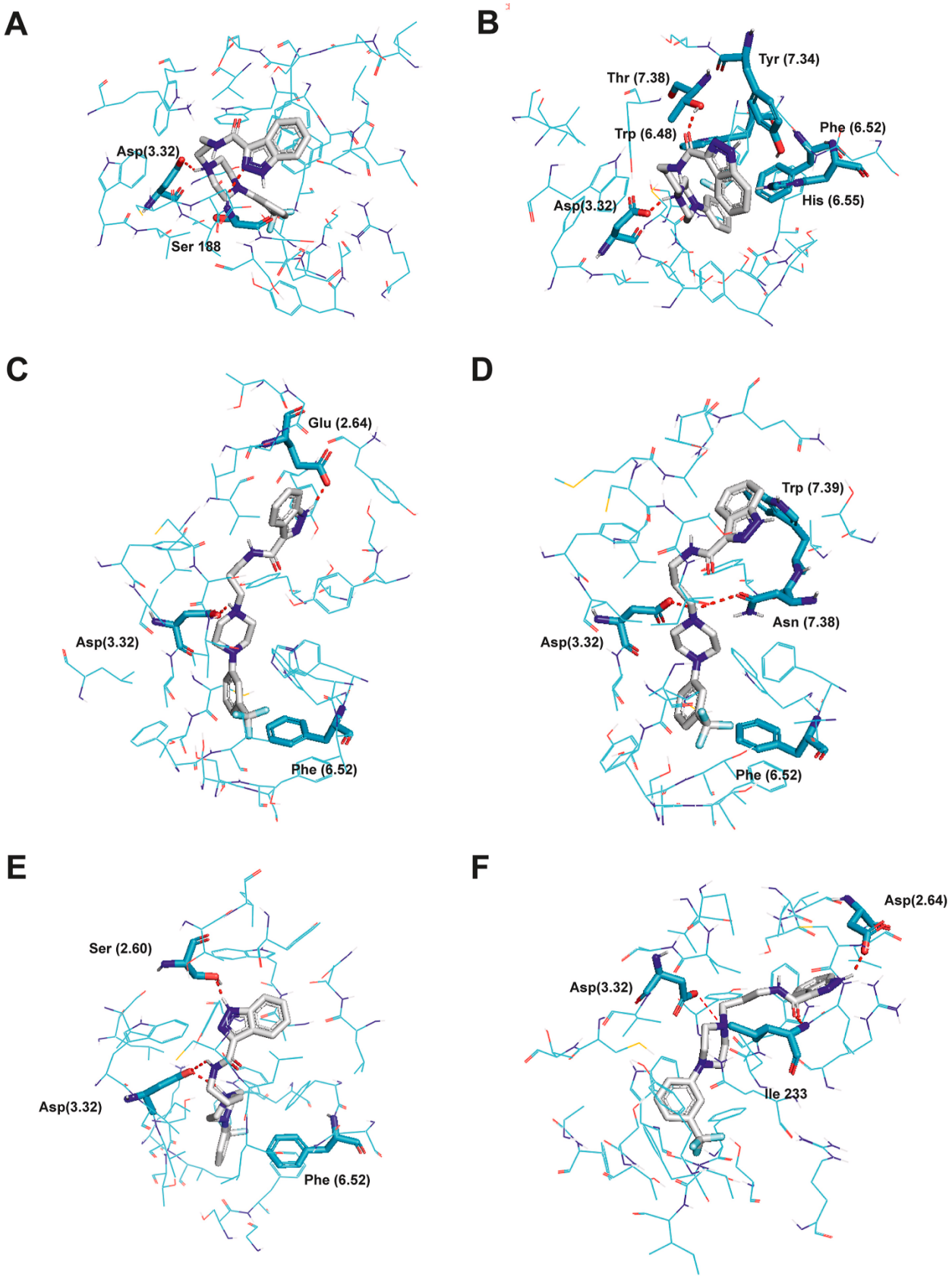
A
Asp(3.32)
Ser 188
B
Tyr (7.34)
Thr (7.38)
Trp (6.48)
Phe (6.52)
His (6.55)
Asp(3.32)
C
Glu (2.64)
Asp(3.32)
Phe (6.52)
D
Trp (7.39)
Asn (7.38)
Asp(3.32)
Phe (6.52)
E
Ser (2.60)
Asp(3.32)
Phe (6.52)
F
Asp(2.64)
Asp(3.32)
Ile 233

Fig. 5.

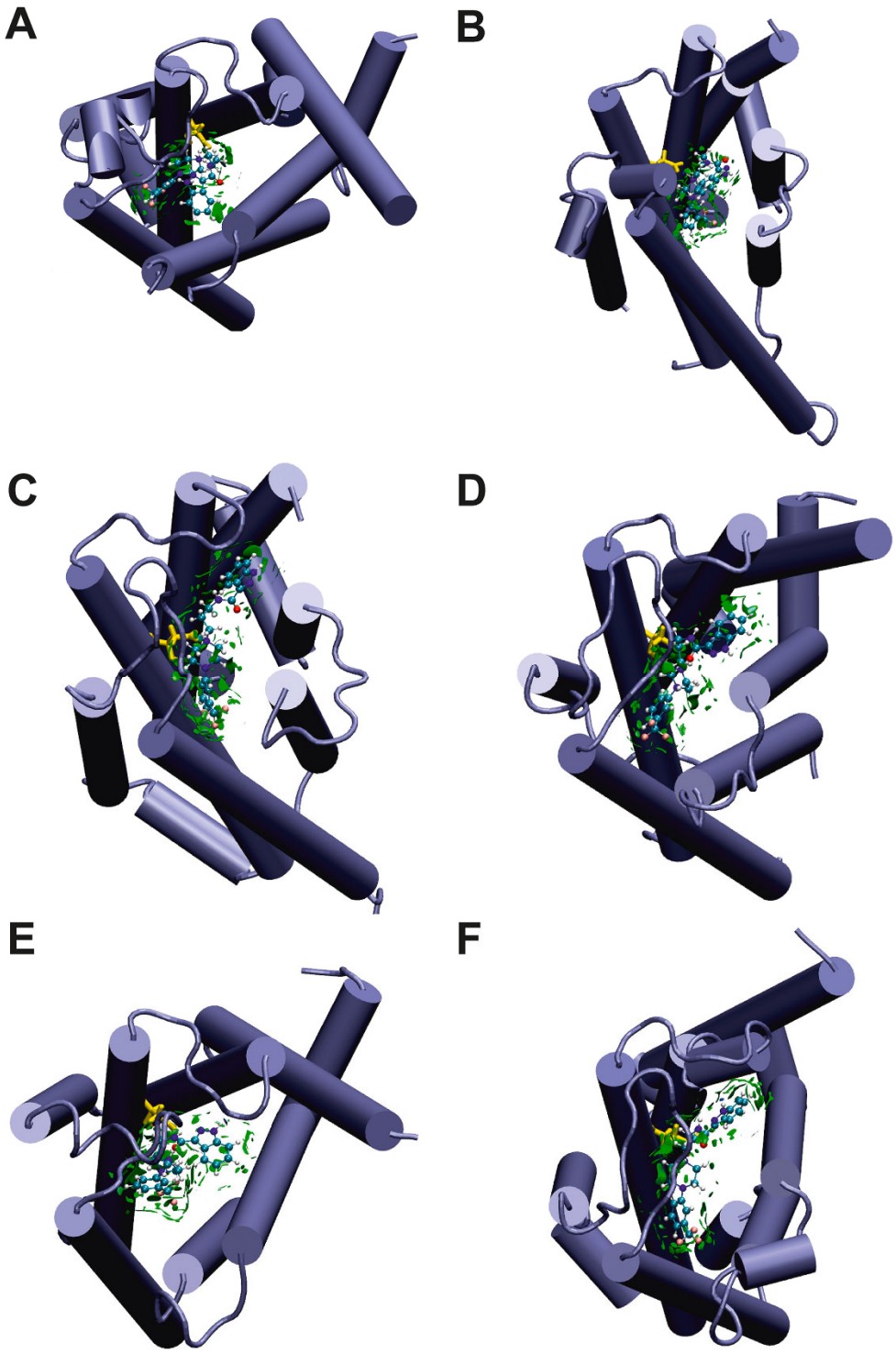

Fig. 6.

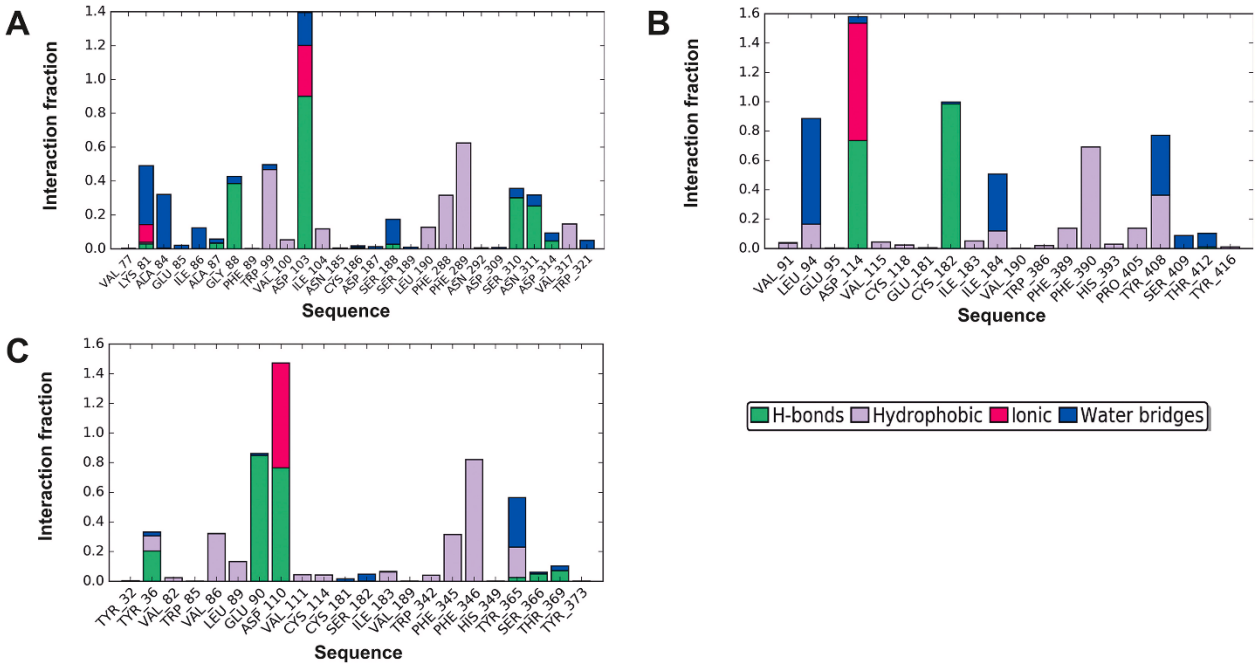
A
Interaction fraction
Sequence
B
Interaction fraction
Sequence
C
Interaction fraction
Sequence
H-bonds
Hydrophobic
Ionic
Water bridges

Fig. 7.

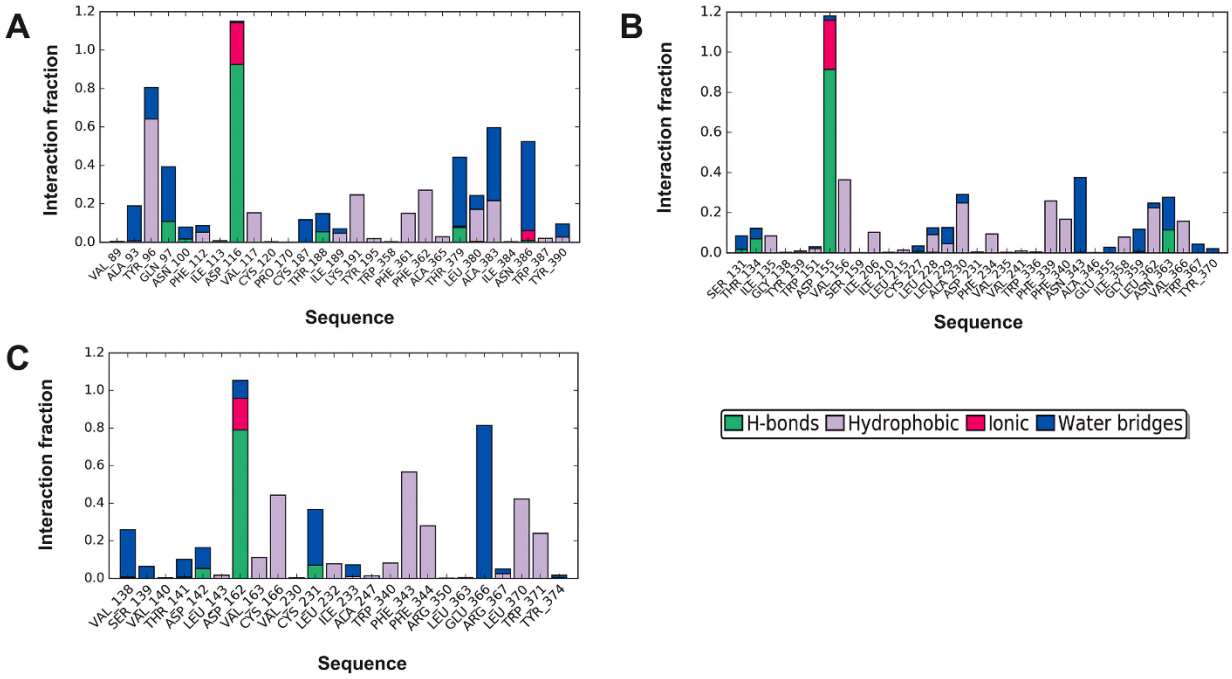
A
B
C
Interaction fraction
Sequence
H-bonds
Hydrophobic
Ionic
Water bridges

Fig. 8.

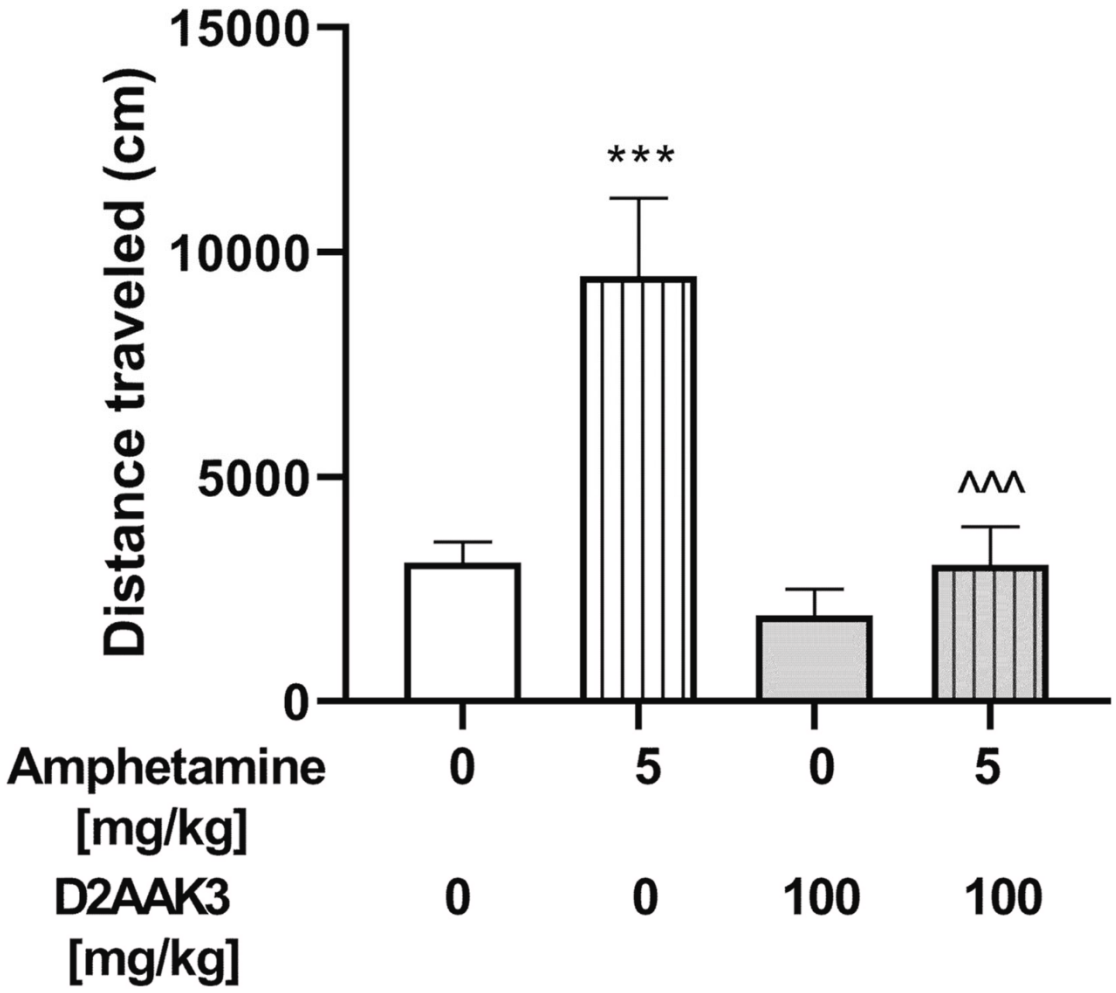
15000
10000
5000
0
Distance traveled (cm)
***
^^^
Amphetamine [mg/kg]
0
5
0
5
D2AAK3 [mg/kg]
0
0
100
100

Fig. 9.

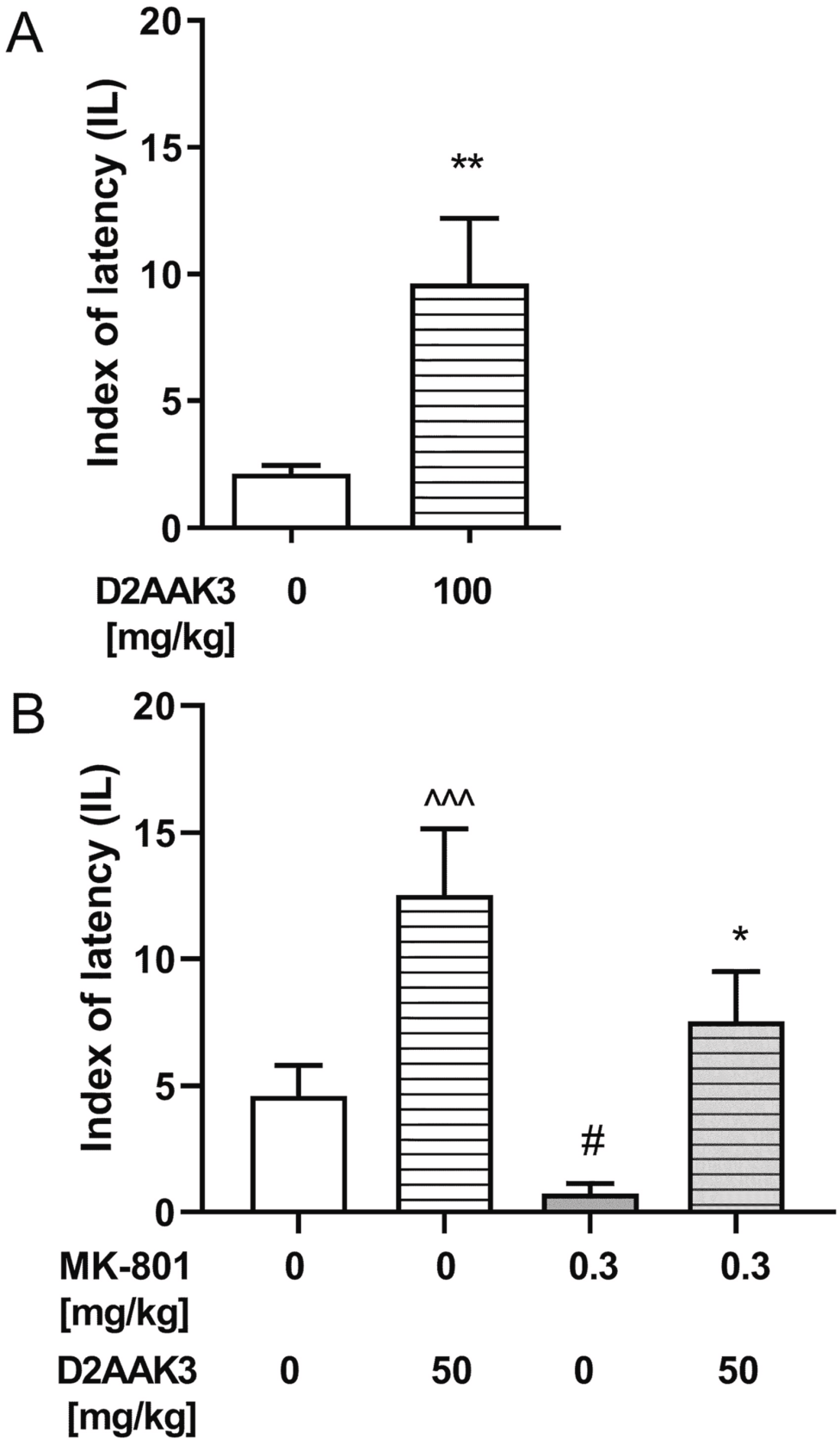
A
Index of latency (IL)
20
15
10
5
0
**
D2AAK3 [mg/kg]
0
100
B
Index of latency (IL)
20
15
10
5
0
^^^
#
*
MK-801 [mg/kg]
0
0
0.3
0.3
D2AAK3 [mg/kg]
0
50
0
50

Fig. 10.

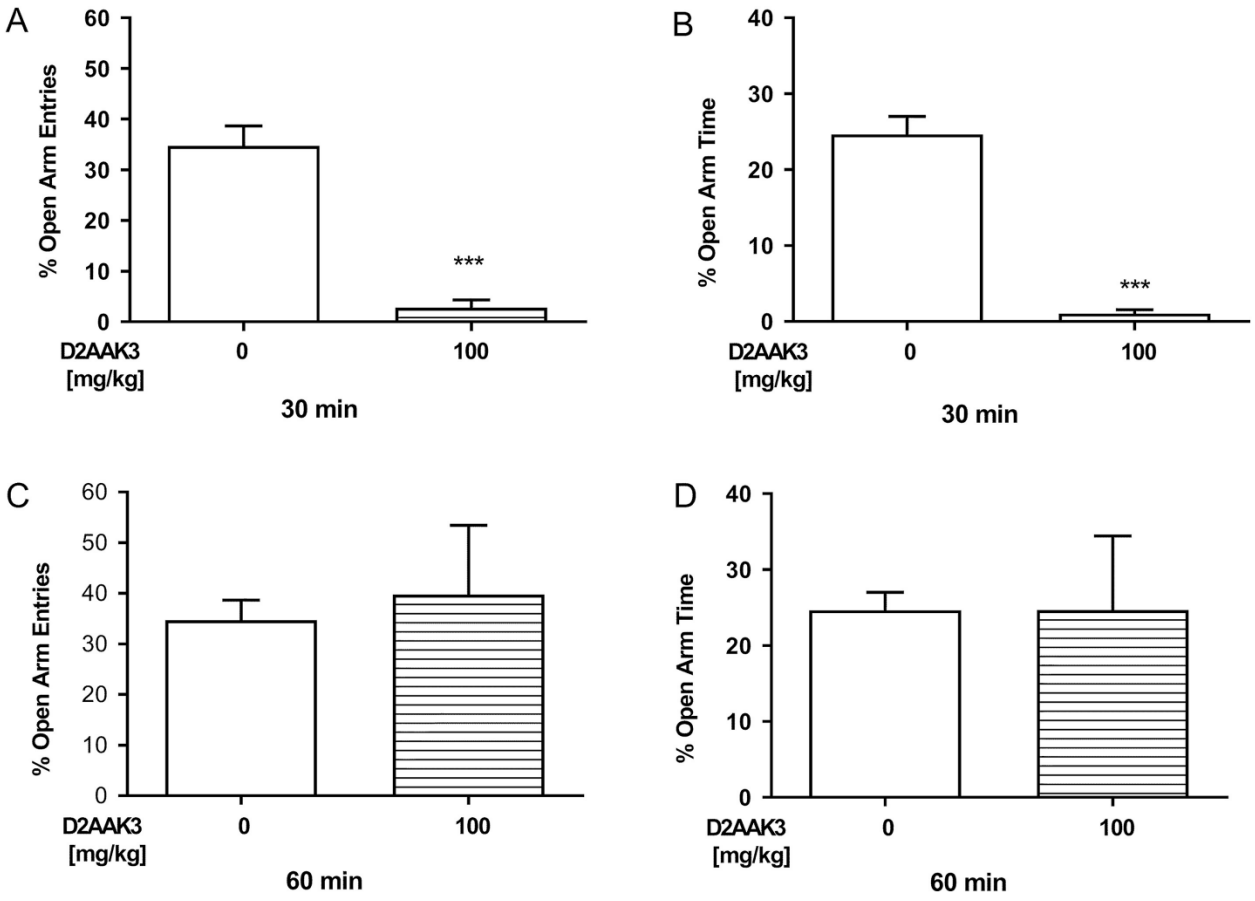
A
% Open Arm Entries
60
50
40
30
20
10
0
***
D2AAK3
[mg/kg]
0
100
30 min
B
% Open Arm Time
40
30
20
10
0
***
D2AAK3
[mg/kg]
0
100
30 min
C
% Open Arm Entries
60
50
40
30
20
10
0
D2AAK3
[mg/kg]
0
100
60 min
D
% Open Arm Time
40
30
20
10
0
D2AAK3
[mg/kg]
0
100
60 min

Table 1. Experimental radioligand binding data for D2AAK3.

	pK_i (K_i) or % inh. at 10 μM[a]							
Comp.	***h*D$_2$**	***h*D$_1$**	***h*D$_3$**	***h*5-HT$_{1A}$**	***h*5-HT$_{2A}$**	***h*5-HT$_7$**	***h*H$_1$**	***h*M$_1$**
D2AAK3	6.94 ± 0.06 (115)	6.33 ± 0.01 (469)	6.26 ± 0.01 (551)	7.34 ± 0.14 (51.4)	6.88 ± 0.23 (151)	6.09 ± 0.03 (807)	6.36 ± 0.11 (433)	5.19 ± 0.02[b] (~6442)
Haloperidol	8.30 ± 0.07 (5.22)	7.93 ± 0.02 (11.8)	8.00 ± 0.08 (10.5)	ND[c]	ND	ND	ND	ND
5-CT[d]	ND	ND	ND	9.00 ± 0.06 (1.04)	ND	ND	ND	ND
Methysergide	ND	ND	ND	ND	9.29 ± 0.07 (0.53)	ND	ND	ND
Clozapine	ND	ND	ND	ND	ND	6.20 ± 0.05 (632)	ND	ND
Doxepin	ND	ND	ND	ND	ND	ND	9.26 ± 0.18 (0.55)	ND
Ipratropium	ND	ND	ND	ND	ND	ND	ND	9.27 ± 0.03 (0.53)

[a] Data are expressed as pK_i (mean ± SEM) and K_i (nM) or % inh. at 10 μM (mean ± SEM) of 2–3 independent experiments performed in duplicate.

[b] Full displacement of specific binding was not achieved at the maximum concentration assayed, so K_i value could be not accurately estimated; maximum displacement achieved (100 μM) was 66%.

[c] ND, not determined. [d] 5-CT, 5-carboxamidotryptamine.

[d] Data for hD$_2$, hD$_1$, hD$_3$, h5-HT$_{1A}$, h5-HT$_{2A}$ were previously reported in Kaczor et al. (2016c).

Table 2. Evaluation of potency and efficacy of compound D2AAK3 at the indicated receptors in *in vitro* functional assays: [a] efficacy (% inh., % of inhibition of dopamine response) and potency (K_B) as D_2 antagonist in cAMP assays (Kaczor et al., 2016a, Kaczor et al., 2016b, Kaczor et al., 2016c, Kaczor et al., 2016d); [b] efficacy (%E_{max}, % of maximal response) and potency (pEC_{50}, -log EC_{50}; EC_{50}, concentration of the compound eliciting the 50% of maximal compound response) as 5-HT_{1A} agonist in cAMP assays; [c] efficacy (% inh., % of inhibition of 5-HT response) and potency (pIC_{50}, -log IC_{50}; IC_{50}, concentration of the compound eliciting the 50% of maximal compound response) as 5-HT_{2A} antagonist in IP assays. Data are mean ± SEM of 2–3 independent experiments performed in duplicate or triplicate.

***h*D$_2$[a]**		***h*5-HT$_{1A}$[b]**			***h*5-HT$_{2A}$[c]**		
% inh. at 10 µM	**K_B [nM]**	**%E_{max}**	**pEC_{50}**	**EC_{50} [nM]**	**% inh. at 10 µM**	**pIC_{50}**	**IC_{50} [nM]**
62.7 ± 2.6%	130.6	92.6 ± 1.2%	5.37 ± 0.09	4246	98.5 ± 1.5%	6.61 ± 0.10	247

Graphical abstract